

Article

A Soliton Solution for the Kadomtsev–Petviashvili Model Using Two Novel Schemes

Asghar Ali ¹, Sara Javed ¹, Muhammad Nadeem ^{2,*}, Loredana Florentina Iambor ^{3,*} and Sorin Mureșan ³

¹ Department of Mathematics, Mirpur University of Science and Technology— (MUST), Mirpur 10250, Azad Jammu and Kashmir, Pakistan; drali@must.edu.pk (A.A.); sarajaved.must@gmail.com (S.J.)

² School of Mathematics and Statistics, Qujing Normal University, Qujing 655011, China

³ Department of Mathematics and Computer Science, University of Oradea, 1 University Street, 410087 Oradea, Romania; smuresan@uoradea.ro

* Correspondence: nadeem@mail.qjnu.edu.cn (M.N.); iambor.loredana@gmail.com (L.F.I.)

Abstract: Symmetries are crucial to the investigation of nonlinear physical processes, particularly the evaluation of a differential problem in the real world. This study focuses on the investigation of the Kadomtsev–Petviashvili (KP) model within a (3+1)-dimensional domain, governing the behavior of wave propagation in a medium characterized by both nonlinearity and dispersion. The inquiry employs two distinct analytical techniques to derive multiple soliton solutions and multiple solitary wave solutions. These methods include the modified Sardar sub-equation technique and the Darboux transformation (DT). The modified Sardar sub-equation technique is used to obtain multiple soliton solutions, while the DT is introduced to develop two bright and two dark soliton solutions. These solutions are presented alongside their corresponding constraint conditions and illustrated through 3-D, 2-D, and contour plots to physically portray the derived solutions. The results demonstrate that the employed analytical techniques are useful and have not yet been explored in the context of the analyzed models. The proposed methodologies are valuable and can be applied to additional nonlinear evolutionary models employed to describe nonlinear physical models within the domain of nonlinear science.

Keywords: (3+1)-dimensional Kadomtseva–Petviashvili model; the modified Sardar sub-equation technique; Darboux transformation; soliton dynamics



Citation: Ali, A.; Javed, S.; Nadeem, M.; Iambor, L.F.; Mureșan, S. A Soliton Solution for the Kadomtsev–Petviashvili Model Using Two Novel Schemes. *Symmetry* **2023**, *15*, 1364. <https://doi.org/10.3390/sym15071364>

Academic Editors: Boris Malomed and Mariano Torrisi

Received: 10 June 2023

Revised: 27 June 2023

Accepted: 3 July 2023

Published: 4 July 2023



Copyright: © 2023 by the authors. Licensee MDPI, Basel, Switzerland. This article is an open access article distributed under the terms and conditions of the Creative Commons Attribution (CC BY) license (<https://creativecommons.org/licenses/by/4.0/>).

1. Introduction

Recently, a higher-dimensional integrable system's physical and mathematical aspects have been addressed. A tremendous amount of research has gone into developing and understanding integrable models because of their major effects in scientific fields. Many investigations have been conducted on higher-dimensional integrable equations in many different sectors, including solitary wave theory and plasma acoustic waves, as well as many more scientific fields. Many soliton solutions can be found in [1–14].

A nonlinear partial differential equation, the (3+1)-dimensional Kadomtsev–Petviashvili (KP) model describes wave events in a four-dimensional space–time context. It is an extension of the (2+1)-dimensional KP model and is applied to the study of many physical systems, such as fluid dynamics, nonlinear optics, and plasma physics. The soliton solutions, which are localized wave packets that can travel through the medium without changing their shape or amplitude, are of great importance in the (3+1)-dimensional KP model. Numerous scientific phenomena, including wave propagation, energy transport, and information encoding, depend heavily on soliton behavior. A (3+1)-dimensional KP model was presented in [1] as

$$\alpha \mathcal{M}_{xt} - \frac{\alpha^4 + \beta^4 - 6\alpha^2\beta^2}{16} \mathcal{M}_{xxxx} - \frac{3(\beta^2 - \alpha^2)}{4} (\mathcal{M}^2)_{xx} - \frac{3}{4} \mathcal{M}_{yy} + \frac{3}{4} \mathcal{M}_{zz} = 0, \quad (1)$$

which allows for a weak dispersion factor \mathcal{M}_{xxxx} . Its integrability was examined by using the Bäcklund transformation in Equation (1). The suggested version of Equation (1) is not in the form of Painlevé integrability. To expand and generalize integrable systems to larger-dimensional models, researchers have conducted a lot of work. The development of numerous higher-dimensionally integrable systems is the result of these efforts. Through the application of a number of potent approaches, the higher-order integrable model enables the determination of the dynamic behavior of the solution. Recently, there have been two thorough reviews of the subject of nonlinear wave structures in various physical contexts, including consideration of nonlinear optics, photonics, and matter waves in Einstein Bose and the condensation products [15,16]. Addressing the context of liquid crystals, molecular Einstein's condensates, photonic systems, and other fundamental contexts, researchers have examined the two- and three-dimensional resonances and associated states, such as quantum droplets [17]. In addition, new information on light bullets, the generation of few-cycle (ultra-narrow) optical pulses and their many uses, and the appearance of rogue waves in a variety of media was formally provided in the overview published in [18]. The extended (3+1)-dimensional Painlevé integrable equation is now examined as:

$$\alpha \mathcal{M}_{xt} - \frac{\alpha^4 + \beta^4 - 6\alpha^2\beta^2}{16} \mathcal{M}_{xxxx} - \frac{3(\beta^2 - \alpha^2)}{4} (\mathcal{M}^2)_{xx} + a\mathcal{M}_{xx} + b\mathcal{M}_{xy} + c\mathcal{M}_{xz} + d\mathcal{M}_{zz} + e\mathcal{M}_{yz} + \frac{e^2}{4d} \mathcal{M}_{yy} = 0, \quad (2)$$

$$\alpha \mathcal{M}_{xt} - \frac{\alpha^4 + \beta^4 - 6\alpha^2\beta^2}{16} \mathcal{M}_{xxxx} - \frac{3(\beta^2 - \alpha^2)}{4} (\mathcal{M}^2)_{xx} + a\mathcal{M}_{xx} + b\mathcal{M}_{xy} + c\mathcal{M}_{yy} = 0. \quad (3)$$

The majority of phenomena can be represented by nonlinear differential equations (NDEs). Determining an exact solution for nonlinear differential equations is significantly more difficult in this circumstance. Numerous analytical techniques have been employed to solve nonlinear issues, including the Adomian decomposition technique and the variational homotopy perturbation technique, the variational iteration technique, the homotopy perturbation technique, the differential transform technique, and the variational iteration technique.

Additionally, several intriguing techniques have been researched to find precise solutions for nonlinear PDEs, including the prolonged sin-Gordon expansion technique, the modified Tanh-function technique, and the modified Kudryashov technique. For Schamel's equation, accurate nondifferentiable solutions have been found. For nonlinear PDEs defined in the sense of conformable and local fractional derivatives, several of the aforementioned techniques have been attained. The Hirota bilinear technique is perhaps one of the most fascinating exact solution techniques in solution theory for solving nonlinear integrable equations.

Lie group theory plays a significant part in symmetry reduction, whenever the traditional methods for minimizing the number of independent components in a problem are the solution under some subgroup of the symmetry group of that system. Numerous scientists have claimed that finding the approximate solution to such problems is very important either by using numerical or analytical techniques. Therefore, symmetry analysis is a very useful system for identifying PDEs, especially when the equations are derived from the ideas of mathematical accounting. Although symmetry is an essential component of nature, the majority of the findings are not symmetrical. An effective approach for hiding symmetry is to offer unexpected symmetry-breaking phenomena. Discrete and continuous finite symmetries come in two different varieties. Parity and temporal inversion are two examples of natural symmetries that are discrete, whereas space is a continuous transformation.

Each of these techniques has pros and cons. The optimum auxiliary function technique, a novel methodology, has been similarly expanded to partial differential equations (PDEs). Recent years have seen a boom in research on multiple soliton solutions and lump solutions because of their significance in nonlinear scientific domains. High-amplitude localization

is a feature of lumps. The Hirota bilinear form [19–21], can be used to produce lumps and solitons. A lump may physically separate (or emit) from a line soliton, survive for a momentary interval, and then meld with the following soliton. Recently, Wazwaz used this model to explore nonlinear integrable models and a number of potent approaches, including the Hirota method and the Darboux transformation method [22–24]. Darboux transformation is a powerful mathematical technique used in the study of integrable systems and nonlinear partial differential equations. It was first introduced by the French mathematician Gaston Darboux in the late 19th century as a way of constructing new solutions to differential equations from known ones. The Darboux transformation works by converting a given differential equation solution into a new solution that uses the same differential equation but has different boundary conditions. The Darboux matrix, a new function that is used to methodically alter the initial answer, is introduced in order to make this transformation. One of the key benefits of the Darboux transformation is that it enables the building of an endless number of new solutions to a given differential equation, which can provide important information about how the system under study behaves. Numerous physical systems, such as quantum mechanics, fluid dynamics, and nonlinear optics have all been studied using it.

The novelty of this work is that the Darboux transformation and the modified Sardar sub-equation technique are applied to the KP model in this study to evaluate and analyze their impacts. New soliton solutions, new aspects of the model's behavior, or other characteristics that have not yet been investigated in the literature may be found through this approach [25–27]. This paper has the potential to increase knowledge and comprehension in the area of the KP equation by utilizing these methodologies and examining their consequences. It might offer fresh perspectives, illuminate the integrability characteristics, unearth more symmetries, or make known KP model-related events that were previously unknown. The study of systems that can be precisely solved using analytical techniques is the focus of the field of integrable systems, which includes the Darboux transformation as a key tool. It has played a central role in the development of many important mathematical concepts, such as soliton theory and the inverse scattering method [28–30].

In this paper, we use different techniques, the modified Sardar sub-equation technique MSST and DT, to find soliton solutions.

Additionally, we improve the discussion on the theoretical implications of our research. We illustrate our ability to achieve significant theoretical advancement by describing the exact analytical framework used and highlighting the innovative methods used, such as the MSST and DT. With the help of these innovations, we identify new solitons, which are essential for comprehending the behavior of the (3+1)-dimensional KP model. The discussion of the potential applications resulting from the derived soliton solutions is expanded. Numerous disciplines are included in these applications, including wave phenomena, nonlinear optics, fluid dynamics, and plasma physics.

The layout of the paper is as follows: Section 2 explains the general description of the used techniques and the application of the governing model. In Section 3, we discuss the DT of the given model. The results and discussion are provided in Section 4. Section 5 provides the conclusion.

2. General Description and Application of the Proposed Methods

This section provides a detailed explanation of the methodology used for Equation (PDE) to produce soliton solutions. The following form is the generic NLPDE:

$$\mathcal{S}(w, w_x, w_t, w_{xx}, w_{xt}, \dots) = 0, \quad (4)$$

where $w = w(x, t)$ is an unexplained function. Applying the transformation

$$w(x, t) = \mathcal{W}(\tau), \quad \tau = x - vt, \quad (5)$$

Equation (1) can be changed into an ODE, as

$$\mathcal{R}(W, W', W'', \dots) = 0, \quad (6)$$

where v and W' represent the constant velocity and $\frac{dw}{d\tau}$, respectively.

The methodology is described in the following subsection.

2.1. The Modified Sardar Sub-Equation Technique

The given form describes the general solution of Equation (6), as per the method.

$$W(\tau) = R_0 + \sum_{i=1}^N R_i \mathcal{P}^i(\tau), \quad R_i \neq 0, \quad (7)$$

where $W = W(\tau)$, and the following equation is the first-order differential equation that satisfies the general solution to Equation (7).

$$\mathcal{P}'(\tau)^2 = \epsilon_2 \mathcal{P}(\tau)^4 + \epsilon_1 \mathcal{P}(\tau)^2 + \epsilon_0, \quad (8)$$

where $\epsilon_0 \neq 1$ and ϵ_1 and $\epsilon_2 \neq 0$ are integers. We calculate the constants R_0 , R_1 , and R_2 , and additionally, it is possible for R_i to be zero. We determine the value of N using the balance principle. Following are the solutions to Equation (8).

Case 1:

- If $\epsilon_0 = 0, \epsilon_1 > 0$, and $\epsilon_2 \neq 0$, then

$$\mathcal{P}_1(\tau) = \sqrt{-\frac{\epsilon_1}{\epsilon_2}} \operatorname{sech}(\sqrt{\epsilon_1}(\eta + \tau)), \quad (9)$$

- If $\epsilon_0 = 0, \epsilon_1 > 0$, and $\epsilon_2 \neq 0$, then

$$\mathcal{P}_2(\tau) = \sqrt{-\frac{\epsilon_1}{\epsilon_2}} \operatorname{csch}(\sqrt{\epsilon_1}(\eta + \tau)). \quad (10)$$

Case 2:

- For constants f_1 and f_2 , let $\epsilon_0 = 0, \epsilon_1 > 0$, and $\epsilon_2 = +4f_1f_2$; then,

$$\mathcal{P}_3(\zeta) = \frac{4f_1\sqrt{\epsilon_1}}{(4f_1^2 - \epsilon_2) \sinh(\sqrt{\epsilon_1}(\eta + \tau)) + (4f_1^2 - \epsilon_2) \cosh(\sqrt{\epsilon_1}(\eta + \tau))}. \quad (11)$$

Case 3:

- For constants R_1 and R_2 , let $\epsilon_0 = \frac{\epsilon_1^2}{4\epsilon_2}, \epsilon_1 < 0$, and $\epsilon_2 > 0$; then,

$$\mathcal{P}_4(\tau) = \sqrt{-\frac{\epsilon_1}{2\epsilon_2}} \tanh\left(\sqrt{-\frac{\epsilon_1}{2}}(\eta + \tau)\right). \quad (12)$$

- For constants R_1 and R_2 , let $\epsilon_0 = \frac{\epsilon_1^2}{4\epsilon_2}, \epsilon_1 < 0$, and $\epsilon_2 > 0$; then,

$$\mathcal{P}_5(\tau) = \sqrt{-\frac{\epsilon_1}{2\epsilon_2}} \coth\left(\sqrt{-\frac{\epsilon_1}{2}}(\eta + \tau)\right). \quad (13)$$

- For constants R_1 and R_2 , let $\epsilon_0 = \frac{\epsilon_1^2}{4\epsilon_2}, \epsilon_1 < 0$, and $\epsilon_2 > 0$; then,

$$\mathcal{P}_6(\tau) = \sqrt{-\frac{\epsilon_1}{2\epsilon_2}} \left(\tanh\left(\sqrt{-\frac{\epsilon_1}{2}}(\eta + \tau)\right) + i \operatorname{sech}\left(\sqrt{-2\epsilon_1}(\eta + \tau)\right) \right). \quad (14)$$

- For constants R_1 and R_2 , let $\epsilon_0 = \frac{\epsilon_1^2}{4\epsilon_2}$, $\epsilon_1 < 0$, and $\epsilon_2 > 0$; then,

$$\mathcal{P}_7(\tau) = \sqrt{-\frac{\epsilon_1}{8\epsilon_2}} \left(\tanh\left(\sqrt{-\frac{\epsilon_1}{8}}(\eta + \tau)\right) + \coth\left(\sqrt{-\frac{\epsilon_1}{8}}(\eta + \tau)\right) \right). \tag{15}$$

- For constants R_1 and R_2 , let $\epsilon_0 = \frac{\epsilon_1^2}{4\epsilon_2}$, $\epsilon_1 < 0$, and $\epsilon_2 > 0$; then,

$$\mathcal{P}_8(\tau) = \frac{\sqrt{-\frac{\epsilon_1}{2\epsilon_2}} \cosh(\sqrt{-2\epsilon_1}(\eta + \tau))}{\sinh(\sqrt{-2\epsilon_1}(\eta + \tau)) + i}. \tag{16}$$

Case 4:

- Let $\epsilon_0 = 0$, $\epsilon_1 < 0$, and $\epsilon_2 \neq 0$; then,

$$\mathcal{P}_9(\tau) = \sqrt{-\frac{\epsilon_1}{\epsilon_2}} \sec(\sqrt{-\epsilon_1}(\eta + \tau)). \tag{17}$$

- Let $\epsilon_0 = 0$, $\epsilon_1 < 0$, and $\epsilon_2 \neq 0$; then,

$$\mathcal{P}_{10}(\tau) = \sqrt{-\frac{\epsilon_1}{\epsilon_2}} \csc(\sqrt{-\epsilon_1}(\eta + \tau)). \tag{18}$$

Case 5:

- Let $\epsilon_0 = \frac{\epsilon_1^2}{4\epsilon_2}$, $\epsilon_1 > 0$, $\epsilon_2 > 0$, and $R_1^2 - R_2^2 > 0$; then,

$$\mathcal{P}_{11}(\tau) = \sqrt{-\frac{\epsilon_1}{2\epsilon_2}} \tan\left(\sqrt{\frac{\epsilon_1}{2}}(\eta + \tau)\right). \tag{19}$$

- Let $\epsilon_0 = \frac{\epsilon_1^2}{4\epsilon_2}$, $\epsilon_1 > 0$, $\epsilon_2 > 0$, and $R_1^2 - R_2^2 > 0$; then,

$$\mathcal{P}_{12}(\tau) = -\sqrt{-\frac{\epsilon_1}{2\epsilon_2}} \cot\left(\sqrt{\frac{\epsilon_1}{2}}(\eta + \tau)\right). \tag{20}$$

- Let $\epsilon_0 = \frac{\epsilon_1^2}{4\epsilon_2}$, $\epsilon_1 > 0$, $\epsilon_2 > 0$, and $R_1^2 - R_2^2 > 0$; then,

$$\mathcal{P}_{13}(\tau) = -\sqrt{-\frac{\epsilon_1}{2\epsilon_2}} \left(\tan(\sqrt{2\epsilon_1}(\eta + \tau)) - \sec(\sqrt{2\epsilon_1}(\eta + \tau)) \right). \tag{21}$$

- Let $\epsilon_0 = \frac{\epsilon_1^2}{4\epsilon_2}$, $\epsilon_1 > 0$, $\epsilon_2 > 0$, and $R_1^2 - R_2^2 > 0$; then,

$$\mathcal{P}_{14}(\tau) = \sqrt{-\frac{\epsilon_1}{8\epsilon_2}} \left(\tan\left(\sqrt{\frac{\epsilon_1}{8}}(\eta + \tau)\right) - \cot\left(\sqrt{\frac{\epsilon_1}{8}}(\eta + \tau)\right) \right). \tag{22}$$

- Let $\epsilon_0 = \frac{\epsilon_1^2}{4\epsilon_2}$, $\epsilon_1 > 0$, $\epsilon_2 > 0$, and $R_1^2 - R_2^2 > 0$; then,

$$\mathcal{P}_{15}(\tau) = \frac{\sqrt{-\frac{\epsilon_1}{2\epsilon_2}} \left(\sqrt{R_1^2 - R_2^2} - W_1 \cos(\sqrt{2\epsilon_1}(\eta + \tau)) \right)}{R_2 + W_1 \sin(\sqrt{2\epsilon_1}(\eta + \tau))}, \tag{23}$$

$$\mathcal{P}_{16}(\tau) = \frac{\sqrt{-\frac{\epsilon_1}{2\epsilon_2}} \cos(\sqrt{2\epsilon_1}(\eta + \tau))}{\sin(\sqrt{2\epsilon_1}(\eta + \tau)) - 1}. \tag{24}$$

Case 6:

- Let $\epsilon_0 = 0$ and $\epsilon_1 > 0$; then,

$$\mathcal{P}_{17}(\tau) = \frac{4\epsilon_1 e^{\sqrt{\epsilon_1}(\eta+\tau)}}{e^{2\sqrt{\epsilon_1}(\eta+\tau)} - 4\epsilon_1 \epsilon_2}. \quad (25)$$

- Let $\epsilon_0 = 0$ and $\epsilon_1 > 0$; then,

$$\mathcal{P}_{18}(\tau) = \frac{4\epsilon_1 e^{\sqrt{\epsilon_1}(\eta+\tau)}}{1 - 4\epsilon_1 \epsilon_2 e^{2\sqrt{\epsilon_1}(\eta+\tau)}}. \quad (26)$$

Case 7:

- Let $\epsilon_0 = 0, \epsilon_1 = 0$, and $\epsilon_2 > 0$; then,

$$\mathcal{H}_{19}(\tau) = \frac{1}{\sqrt{\epsilon_2}(\eta + \tau)}. \quad (27)$$

- Let $\epsilon_0 = 0, \epsilon_1 = 0$, and $\epsilon_2 > 0$; then,

$$\mathcal{P}_{20}(\tau) = \frac{i}{\sqrt{\epsilon_2}(\eta + \tau)}. \quad (28)$$

2.2. Application of the Modified Sardar Sub-Equation Technique

The extended form of the (3+1)-dimensional Kadomtsev–Petviashvili model reads as

$$\begin{aligned} \alpha \mathcal{M}_{xt} - \frac{\alpha^4 - 6\alpha^2\beta^2 + \beta^4}{16} \mathcal{M}_{xxxx} - \frac{3(\beta^2 - \alpha^2)}{4} (\mathcal{M}^2)_{xx} + a\mathcal{M}_{xx} + b\mathcal{M}_{xy} + c\mathcal{M}_{xz} \\ + d\mathcal{M}_{zz} + e\mathcal{M}_{yz} + \frac{e^2}{4d} \mathcal{M}_{yy} = 0, \end{aligned} \quad (29)$$

where β, a, b, c, d , and e are real coefficients, but $\alpha, d \neq 0$, and $\mathcal{M} = s(x, y, z, t)$ is a function that, with relation to the spatial and temporal variables, is sufficiently differentiable. The modification described by

$$\mathcal{M}(x, y, z, t) = s(\tau), \quad \tau = x + y + z - vt, \quad (30)$$

is used to reduce Equation (1) into the following ordinary differential equation

$$-\frac{\alpha^4 - 6\alpha^2\beta^2 + \beta^4}{16} s'' - \frac{3(\beta^2 - \alpha^2)}{4} s^2 + (a + b + c + d + e + \frac{e^2}{4d} - \alpha v) s = 0, \quad (31)$$

which is second-order nonlinear. Applying the homogeneous balancing principle, we obtain $N = 2$. By utilizing the modified Sardar sub-equation technique, we consider the following form of analytical solution

$$\mathcal{M}(\tau) = R_2 \mathcal{P}(\tau)^2 + R_1 \mathcal{P}(\tau) + R_0. \quad (32)$$

Putting Equation (27) into Equation (26) and utilizing Equation (8), we obtain an algebraic system by equating all the coefficients of the various powers of $(\mathcal{P}(\ll))$ to zero. The following is the solution to the system of algebraic equations.

Family 1:

$$\left. \begin{aligned}
 R_0 &\rightarrow \frac{\epsilon_1(\alpha^6 - 7\alpha^4\beta^2 + 7\alpha^2\beta^4 - \beta^6) - \sqrt{(\epsilon_1^2 - 3\epsilon_0\epsilon_2)(\alpha^6 - 7\alpha^4\beta^2 + 7\alpha^2\beta^4 - \beta^6)^2}}{6(\alpha^2 - \beta^2)^2}, \\
 R_1 \rightarrow 0, R_2 &\rightarrow \frac{\epsilon_2(\alpha^4 - 6\alpha^2\beta^2 + \beta^4)}{2(\alpha^2 - \beta^2)}, \quad a \rightarrow \frac{1}{4} \left(\frac{\sqrt{(\epsilon_1^2 - 3\epsilon_0\epsilon_2)(\alpha^6 - 7\alpha^4\beta^2 + 7\alpha^2\beta^4 - \beta^6)^2}}{\alpha^2 - \beta^2} \right. \\
 &\quad \left. - 4b - 4c - \frac{e^2}{d} - 4d - 4e + 4\alpha v \right) \Bigg\}.
 \end{aligned} \right\} \tag{33}$$

The following solutions have been acknowledged as satisfying Family 1:

Case 1:

- If $\epsilon_0 = 0, \epsilon_1 > 0$, and $\epsilon_2 \neq 0$, then

$$\mathcal{M}_{1,1} = \frac{\epsilon_1(\alpha^6 - 7\alpha^4\beta^2 + 7\alpha^2\beta^4 - \beta^6) - \sqrt{(\epsilon_1^2 - 3\epsilon_0\epsilon_2)(\alpha^6 - 7\alpha^4\beta^2 + 7\alpha^2\beta^4 - \beta^6)^2}}{6(\alpha^2 - \beta^2)^2} - \frac{\epsilon_1(\alpha^4 - 6\alpha^2\beta^2 + \beta^4) \operatorname{sech}^2(\sqrt{\epsilon_1}(\eta - tv + x + y + z))}{2(\alpha^2 - \beta^2)}. \tag{34}$$

- If $\epsilon_0 = 0, \epsilon_1 > 0$, and $\epsilon_2 \neq 0$, then

$$\mathcal{M}_{1,2} = \frac{\epsilon_1(\alpha^6 - 7\alpha^4\beta^2 + 7\alpha^2\beta^4 - \beta^6) - \sqrt{(\epsilon_1^2 - 3\epsilon_0\epsilon_2)(\alpha^6 - 7\alpha^4\beta^2 + 7\alpha^2\beta^4 - \beta^6)^2}}{6(\alpha^2 - \beta^2)^2} - \frac{\epsilon_1(\alpha^4 - 6\alpha^2\beta^2 + \beta^4) \operatorname{csch}^2(\sqrt{\epsilon_1}(\eta - tv + x + y + z))}{2(\alpha^2 - \beta^2)}. \tag{35}$$

Case 2:

- For constants f_1 and f_2 , let $\epsilon_0 = 0, \epsilon_1 > 0$, and $\epsilon_2 = +4f_1f_2$; then,

$$\mathcal{M}_{1,3} = \frac{\epsilon_1(\alpha^6 - 7\alpha^4\beta^2 + 7\alpha^2\beta^4 - \beta^6) - \sqrt{(\epsilon_1^2 - 3\epsilon_0\epsilon_2)(\alpha^6 - 7\alpha^4\beta^2 + 7\alpha^2\beta^4 - \beta^6)^2}}{6(\alpha^2 - \beta^2)^2} + \frac{8f_1^2\epsilon_1\epsilon_2(\alpha^4 - 6\alpha^2\beta^2 + \beta^4)}{(\alpha^2 - \beta^2)((4f_1^2 - \epsilon_2) \sinh(\sqrt{\epsilon_1}(\eta - tv + x + y + z)) + (4f_1^2 - \epsilon_2) \cosh(\sqrt{\epsilon_1}(\eta - tv + x + y + z)))^2}. \tag{36}$$

Case 3:

- For constants R_1 and R_2 , let $\epsilon_0 = \frac{\epsilon_1^2}{4\epsilon_2}, \epsilon_1 < 0$, and $\epsilon_2 > 0$; then,

$$\mathcal{M}_{1,4} = \frac{\epsilon_1(\alpha^6 - 7\alpha^4\beta^2 + 7\alpha^2\beta^4 - \beta^6) - \sqrt{(\epsilon_1^2 - 3\epsilon_0\epsilon_2)(\alpha^6 - 7\alpha^4\beta^2 + 7\alpha^2\beta^4 - \beta^6)^2}}{6(\alpha^2 - \beta^2)^2} - \frac{\epsilon_1(\alpha^4 - 6\alpha^2\beta^2 + \beta^4) \tanh^2\left(\frac{\sqrt{-\epsilon_1}(\eta - tv + x + y + z)}{\sqrt{2}}\right)}{4(\alpha^2 - \beta^2)}. \tag{37}$$

- For constants R_1 and R_2 , let $\epsilon_0 = \frac{\epsilon_1^2}{4\epsilon_2}, \epsilon_1 < 0$, and $\epsilon_2 > 0$; then,

$$\mathcal{M}_{1,5} = \frac{\epsilon_1(\alpha^6 - 7\alpha^4\beta^2 + 7\alpha^2\beta^4 - \beta^6) - \sqrt{(\epsilon_1^2 - 3\epsilon_0\epsilon_2)(\alpha^6 - 7\alpha^4\beta^2 + 7\alpha^2\beta^4 - \beta^6)^2}}{6(\alpha^2 - \beta^2)^2} - \frac{\epsilon_1(\alpha^4 - 6\alpha^2\beta^2 + \beta^4) \operatorname{coth}^2\left(\frac{\sqrt{-\epsilon_1}(\eta - tv + x + y + z)}{\sqrt{2}}\right)}{4(\alpha^2 - \beta^2)}. \tag{38}$$

- For constants R_1 and R_2 , let $\epsilon_0 = \frac{\epsilon_1^2}{4\epsilon_2}$, $\epsilon_1 < 0$, and $\epsilon_2 > 0$; then,

$$\mathcal{M}_{1,6} = \frac{\epsilon_1(\alpha^6 - 7\alpha^4\beta^2 + 7\alpha^2\beta^4 - \beta^6) - \sqrt{(\epsilon_1^2 - 3\epsilon_0\epsilon_2)(\alpha^6 - 7\alpha^4\beta^2 + 7\alpha^2\beta^4 - \beta^6)^2}}{6(\alpha^2 - \beta^2)^2} - \frac{\epsilon_1(\alpha^4 - 6\alpha^2\beta^2 + \beta^4) \left(\tanh\left(\frac{\sqrt{-\epsilon_1}(\eta - tv + x + y + z)}{\sqrt{2}}\right) + \operatorname{isech}\left(\sqrt{2}\sqrt{-\epsilon_1}(\eta - tv + x + y + z)\right) \right)^2}{4(\alpha^2 - \beta^2)}. \tag{39}$$

- For constants R_1 and R_2 , let $\epsilon_0 = \frac{\epsilon_1^2}{4\epsilon_2}$, $\epsilon_1 < 0$, and $\epsilon_2 > 0$; then,

$$\mathcal{M}_{1,7} = \frac{\epsilon_1(\alpha^6 - 7\alpha^4\beta^2 + 7\alpha^2\beta^4 - \beta^6) - \sqrt{(\epsilon_1^2 - 3\epsilon_0\epsilon_2)(\alpha^6 - 7\alpha^4\beta^2 + 7\alpha^2\beta^4 - \beta^6)^2}}{6(\alpha^2 - \beta^2)^2} - \frac{\epsilon_1(\alpha^4 - 6\alpha^2\beta^2 + \beta^4) \left(\tanh\left(\frac{\sqrt{-\epsilon_1}(\eta - tv + x + y + z)}{2\sqrt{2}}\right) + \operatorname{coth}\left(\frac{\sqrt{-\epsilon_1}(\eta - tv + x + y + z)}{2\sqrt{2}}\right) \right)^2}{16(\alpha^2 - \beta^2)}. \tag{40}$$

- For constants R_1 and R_2 , let $\epsilon_0 = \frac{\epsilon_1^2}{4\epsilon_2}$, $\epsilon_1 < 0$, and $\epsilon_2 > 0$; then,

$$\mathcal{M}_{1,8} = \frac{\epsilon_1(\alpha^6 - 7\alpha^4\beta^2 + 7\alpha^2\beta^4 - \beta^6) - \sqrt{(\epsilon_1^2 - 3\epsilon_0\epsilon_2)(\alpha^6 - 7\alpha^4\beta^2 + 7\alpha^2\beta^4 - \beta^6)^2}}{6(\alpha^2 - \beta^2)^2} - \frac{\epsilon_1(\alpha^4 - 6\alpha^2\beta^2 + \beta^4) \operatorname{cosh}^2\left(\sqrt{2}\sqrt{-\epsilon_1}(\eta - tv + x + y + z)\right)}{4(\alpha^2 - \beta^2) \left(\sinh\left(\sqrt{2}\sqrt{-\epsilon_1}(\eta - tv + x + y + z)\right) + i \right)^2}. \tag{41}$$

Case 4:

- Let $\epsilon_0 = 0$, $\epsilon_1 < 0$, and $\epsilon_2 \neq 0$; then,

$$\mathcal{M}_{1,9} = \frac{\epsilon_1(\alpha^6 - 7\alpha^4\beta^2 + 7\alpha^2\beta^4 - \beta^6) - \sqrt{(\epsilon_1^2 - 3\epsilon_0\epsilon_2)(\alpha^6 - 7\alpha^4\beta^2 + 7\alpha^2\beta^4 - \beta^6)^2}}{6(\alpha^2 - \beta^2)^2} - \frac{\epsilon_1(\alpha^4 - 6\alpha^2\beta^2 + \beta^4) \operatorname{sec}^2(\sqrt{-\epsilon_1}(\eta - tv + x + y + z))}{2(\alpha^2 - \beta^2)}. \tag{42}$$

- Let $\epsilon_0 = 0$, $\epsilon_1 < 0$, and $\epsilon_2 \neq 0$; then,

$$\mathcal{M}_{1,10} = \frac{\epsilon_1(\alpha^6 - 7\alpha^4\beta^2 + 7\alpha^2\beta^4 - \beta^6) - \sqrt{(\epsilon_1^2 - 3\epsilon_0\epsilon_2)(\alpha^6 - 7\alpha^4\beta^2 + 7\alpha^2\beta^4 - \beta^6)^2}}{6(\alpha^2 - \beta^2)^2} - \frac{\epsilon_1(\alpha^4 - 6\alpha^2\beta^2 + \beta^4) \operatorname{csc}^2(\sqrt{-\epsilon_1}(\eta - tv + x + y + z))}{2(\alpha^2 - \beta^2)}. \tag{43}$$

Case 5:

- Let $\epsilon_0 = \frac{\epsilon_1^2}{4\epsilon_2}$, $\epsilon_1 > 0$, $\epsilon_2 > 0$, and $R_1^2 - R_2^2 > 0$; then,

$$\mathcal{M}_{1,11} = \frac{\epsilon_1(\alpha^6 - 7\alpha^4\beta^2 + 7\alpha^2\beta^4 - \beta^6) - \sqrt{(\epsilon_1^2 - 3\epsilon_0\epsilon_2)(\alpha^6 - 7\alpha^4\beta^2 + 7\alpha^2\beta^4 - \beta^6)^2}}{6(\alpha^2 - \beta^2)^2} - \frac{\epsilon_1(\alpha^4 - 6\alpha^2\beta^2 + \beta^4) \tan^2\left(\frac{\sqrt{\epsilon_1}(\eta - tv + x + y + z)}{\sqrt{2}}\right)}{4(\alpha^2 - \beta^2)}. \tag{44}$$

- Let $\epsilon_0 = \frac{\epsilon_1^2}{4\epsilon_2}, \epsilon_1 > 0, \epsilon_2 > 0,$ and $R_1^2 - R_2^2 > 0;$ then,

$$\mathcal{M}_{1,12} = \frac{\epsilon_1(\alpha^6 - 7\alpha^4\beta^2 + 7\alpha^2\beta^4 - \beta^6) - \sqrt{(\epsilon_1^2 - 3\epsilon_0\epsilon_2)(\alpha^6 - 7\alpha^4\beta^2 + 7\alpha^2\beta^4 - \beta^6)^2}}{6(\alpha^2 - \beta^2)^2} - \frac{\epsilon_1(\alpha^4 - 6\alpha^2\beta^2 + \beta^4) \cot^2\left(\frac{\sqrt{\epsilon_1}(\eta - tv + x + y + z)}{\sqrt{2}}\right)}{4(\alpha^2 - \beta^2)}. \tag{45}$$

- Let $\epsilon_0 = \frac{\epsilon_1^2}{4\epsilon_2}, \epsilon_1 > 0, \epsilon_2 > 0,$ and $R_1^2 - R_2^2 > 0;$ then,

$$\mathcal{M}_{1,13} = \frac{\epsilon_1(\alpha^6 - 7\alpha^4\beta^2 + 7\alpha^2\beta^4 - \beta^6) - \sqrt{(\epsilon_1^2 - 3\epsilon_0\epsilon_2)(\alpha^6 - 7\alpha^4\beta^2 + 7\alpha^2\beta^4 - \beta^6)^2}}{6(\alpha^2 - \beta^2)^2} - \frac{\epsilon_1(\alpha^4 - 6\alpha^2\beta^2 + \beta^4) \left(\tan\left(\sqrt{2}\sqrt{\epsilon_1}(\eta - tv + x + y + z)\right) - \sec\left(\sqrt{2}\sqrt{\epsilon_1}(\eta - tv + x + y + z)\right) \right)^2}{4(\alpha^2 - \beta^2)}. \tag{46}$$

- Let $\epsilon_0 = \frac{\epsilon_1^2}{4\epsilon_2}, \epsilon_1 > 0, \epsilon_2 > 0,$ and $R_1^2 - R_2^2 > 0;$ then,

$$\mathcal{M}_{1,14} = \frac{\epsilon_1(\alpha^6 - 7\alpha^4\beta^2 + 7\alpha^2\beta^4 - \beta^6) - \sqrt{(\epsilon_1^2 - 3\epsilon_0\epsilon_2)(\alpha^6 - 7\alpha^4\beta^2 + 7\alpha^2\beta^4 - \beta^6)^2}}{6(\alpha^2 - \beta^2)^2} - \frac{\epsilon_1(\alpha^4 - 6\alpha^2\beta^2 + \beta^4) \left(\tan\left(\frac{\sqrt{\epsilon_1}(\eta - tv + x + y + z)}{2\sqrt{2}}\right) - \cot\left(\frac{\sqrt{\epsilon_1}(\eta - tv + x + y + z)}{2\sqrt{2}}\right) \right)^2}{16(\alpha^2 - \beta^2)}. \tag{47}$$

- Let $\epsilon_0 = \frac{\epsilon_1^2}{4\epsilon_2}, \epsilon_1 > 0, \epsilon_2 > 0,$ and $R_1^2 - R_2^2 > 0;$ then,

$$\mathcal{M}_{1,15} = \frac{\epsilon_1(\alpha^6 - 7\alpha^4\beta^2 + 7\alpha^2\beta^4 - \beta^6) - \sqrt{(\epsilon_1^2 - 3\epsilon_0\epsilon_2)(\alpha^6 - 7\alpha^4\beta^2 + 7\alpha^2\beta^4 - \beta^6)^2}}{6(\alpha^2 - \beta^2)^2} - \frac{\epsilon_1(\alpha^4 - 6\alpha^2\beta^2 + \beta^4) \left(\frac{1}{2} \sqrt{-\frac{\epsilon_2^2(\alpha^4 - 6\alpha^2\beta^2 + \beta^4)^2}{(\alpha^2 - \beta^2)^2}} - W_1 \cos\left(\sqrt{2}\sqrt{\epsilon_1}(\eta - tv + x + y + z)\right) \right)^2}{4(\alpha^2 - \beta^2) \left(\frac{\epsilon_2(\alpha^4 - 6\alpha^2\beta^2 + \beta^4)}{2(\alpha^2 - \beta^2)} + W_1 \sin\left(\sqrt{2}\sqrt{\epsilon_1}(\eta - tv + x + y + z)\right) \right)^2}. \tag{48}$$

$$\mathcal{M}_{1,16} = \frac{\epsilon_1(\alpha^6 - 7\alpha^4\beta^2 + 7\alpha^2\beta^4 - \beta^6) - \sqrt{(\epsilon_1^2 - 3\epsilon_0\epsilon_2)(\alpha^6 - 7\alpha^4\beta^2 + 7\alpha^2\beta^4 - \beta^6)^2}}{6(\alpha^2 - \beta^2)^2} - \frac{\epsilon_1(\alpha^4 - 6\alpha^2\beta^2 + \beta^4) \cos^2\left(\sqrt{2}\sqrt{\epsilon_1}(\eta - tv + x + y + z)\right)}{4(\alpha^2 - \beta^2) \left(\sin\left(\sqrt{2}\sqrt{\epsilon_1}(\eta - tv + x + y + z)\right) - 1 \right)^2}. \tag{49}$$

Case 6:

- Let $\epsilon_0 = 0$ and $\epsilon_1 > 0$; then,

$$\mathcal{M}_{1,17} = \frac{\epsilon_1(\alpha^6 - 7\alpha^4\beta^2 + 7\alpha^2\beta^4 - \beta^6) - \sqrt{(\epsilon_1^2 - 3\epsilon_0\epsilon_2)(\alpha^6 - 7\alpha^4\beta^2 + 7\alpha^2\beta^4 - \beta^6)^2}}{6(\alpha^2 - \beta^2)^2} + \frac{8\epsilon_2\epsilon_1^2(\alpha^4 - 6\alpha^2\beta^2 + \beta^4)e^{2\sqrt{\epsilon_1}(\eta - tv + x + y + z)}}{(\alpha^2 - \beta^2)(e^{2\sqrt{\epsilon_1}(\eta - tv + x + y + z)} - 4\epsilon_1\epsilon_2)^2}. \tag{50}$$

- Let $\epsilon_0 = 0$ and $\epsilon_1 > 0$; then,

$$\mathcal{M}_{1,18} = \frac{\epsilon_1(\alpha^6 - 7\alpha^4\beta^2 + 7\alpha^2\beta^4 - \beta^6) - \sqrt{(\epsilon_1^2 - 3\epsilon_0\epsilon_2)(\alpha^6 - 7\alpha^4\beta^2 + 7\alpha^2\beta^4 - \beta^6)^2}}{6(\alpha^2 - \beta^2)^2} + \frac{8\epsilon_2\epsilon_1^2(\alpha^4 - 6\alpha^2\beta^2 + \beta^4)e^{2\sqrt{\epsilon_1}(\eta - tv + x + y + z)}}{(\alpha^2 - \beta^2)(1 - 4\epsilon_1\epsilon_2e^{2\sqrt{\epsilon_1}(\eta - tv + x + y + z)})^2}. \tag{51}$$

Case 7:

- Let $\epsilon_0 = 0, \epsilon_1 = 0$, and $\epsilon_2 > 0$; then,

$$\mathcal{M}_{1,19} = \frac{\epsilon_1(\alpha^6 - 7\alpha^4\beta^2 + 7\alpha^2\beta^4 - \beta^6) - \sqrt{(\epsilon_1^2 - 3\epsilon_0\epsilon_2)(\alpha^6 - 7\alpha^4\beta^2 + 7\alpha^2\beta^4 - \beta^6)^2}}{6(\alpha^2 - \beta^2)^2} + \frac{\alpha^4 - 6\alpha^2\beta^2 + \beta^4}{2(\alpha^2 - \beta^2)(\eta - tv + x + y + z)^2}. \tag{52}$$

- Let $\epsilon_0 = 0, \epsilon_1 = 0$, and $\epsilon_2 > 0$; then,

$$\mathcal{M}_{1,20} = \frac{\epsilon_1(\alpha^6 - 7\alpha^4\beta^2 + 7\alpha^2\beta^4 - \beta^6) - \sqrt{(\epsilon_1^2 - 3\epsilon_0\epsilon_2)(\alpha^6 - 7\alpha^4\beta^2 + 7\alpha^2\beta^4 - \beta^6)^2}}{6(\alpha^2 - \beta^2)^2} - \frac{\alpha^4 - 6\alpha^2\beta^2 + \beta^4}{2(\alpha^2 - \beta^2)(\eta - tv + x + y + z)^2}. \tag{53}$$

3. Darboux Transformation

The corresponding Lax representation of Equation (1) takes the form:

$$\Psi_x = V\Psi, \quad \Psi_t = (2\alpha\mu + 4\beta\mu^2)\Psi_y + (+6\alpha\mu^3)\Psi_z + U\Psi, \tag{54}$$

in which

$$V = -i\mu\omega_1 + V_0, \quad U = \mu U_1 + U_0 + \frac{i}{\mu + \gamma} U_{-1},$$

$$\omega_1 = \begin{pmatrix} 1 & 0 \\ 0 & -1 \end{pmatrix}, \quad V_0 = \begin{pmatrix} 0 & m \\ -n & 0 \end{pmatrix}, \quad U_{-1} = \begin{pmatrix} \xi & -l \\ -q & \xi \end{pmatrix},$$

$$U_1 = \gamma\omega_1 + 2i\beta\omega_1 V_{0y}, \quad U_0 = -\frac{i}{2}u\omega_1 + \begin{pmatrix} 0 & -\alpha m_y - \beta m_{xy} + i\gamma m \\ i\alpha n_y + \beta n_{xy} - i\gamma n & 0 \end{pmatrix}.$$

If λ is a complex spectral parameter that is independent of time (t), then $\Psi = \Psi(x, t) = (\psi(x, t), \phi(x, t))^T$ (T) denote the transpose of the complex eigenfunctions. The zero curva-

tures equation $V_t - U_x + [V, U] = 0$, where V and U are 2×2 matrices that meet the linear isospectral problem, is identical to Equation (1). According to Equation (54), the Lax pair of Equation (1) is:

$$\Psi = V\Psi, \quad V = \begin{pmatrix} -i\mu & m \\ -\sigma m^* & i\mu \end{pmatrix}, \tag{55}$$

$$\Psi_t = U\Psi, \quad U = \begin{pmatrix} \frac{i\zeta}{\mu+\gamma} & -\frac{i}{2(\zeta+\gamma)}m_t \\ -\frac{i\sigma}{2(\zeta+\gamma)}m_t^* & -\frac{i\zeta}{\mu+\gamma} \end{pmatrix}. \tag{56}$$

3.1. The N-Fold DT

The *N-fold* DT of (1) is developed in this section. First, we apply the gauge modification, shown as follows.

$$\tilde{\Psi} = \mathcal{T}\Psi, \tag{57}$$

whereas Ψ satisfies the Lax pairs Equations (55) and (56), \mathcal{T} is a 2×2 Darboux matrix, which is provided here, and $\tilde{\Psi} = \tilde{\Psi}(x, t) = (\tilde{\phi}(x, t), \tilde{\varphi}(x, t))^T$ should maintain the same shape as the Lax pairing. Equations (4) and (5), excluding the replacement of V and U with \tilde{V} and \tilde{U} , are

$$\tilde{\Psi}_x = \tilde{V}\tilde{\Psi}, \quad \tilde{V} = \begin{pmatrix} -i\mu & \tilde{m} \\ -\sigma\tilde{m}^* & i\mu \end{pmatrix}, \tag{58}$$

$$\tilde{\Psi}_t = \tilde{U}\tilde{\Psi}, \quad \tilde{U} = \begin{pmatrix} \frac{i\tilde{\zeta}}{\mu+\gamma} & -\frac{i}{2(\mu+\gamma)}\frac{\partial\tilde{m}}{\partial t} \\ -\frac{i\sigma}{2(\mu+\gamma)}\frac{\partial\tilde{m}^*}{\partial t} & -\frac{i\tilde{\zeta}}{\mu+\gamma} \end{pmatrix}, \tag{59}$$

where $\tilde{m} = \tilde{m}(x, t)$, and $\tilde{\zeta} = \tilde{\zeta}(x, t)$ are novel prospective capabilities that can also address Equation (1). Using Equations (55)–(59), we have

$$\tilde{V} = (\mathcal{T}_x + \mathcal{T}V)\mathcal{T}^{-1}, \quad \tilde{U} = (\mathcal{T}_t + \mathcal{T}U)\mathcal{T}^{-1}, \tag{60}$$

wherein we deduce

$$\tilde{V}_t - \tilde{U}_x + \tilde{V}\tilde{U} - \tilde{U}\tilde{V} = \mathcal{T}(V_t - U_x + VU - UV)\mathcal{T}^{-1}, \tag{61}$$

considering that the equation for zero curvature $V_t - U_x + VU - UV$ in the Darboux matrices is zero \mathcal{T} , that is, nonsingular. So, $\tilde{V}_t - \tilde{U}_x + \tilde{V}\tilde{U} - \tilde{U}\tilde{V} = 0$, and it can also provide the same Equation (1) in $m, \zeta \rightarrow \tilde{m}, \tilde{\zeta}$, i.e., $\tilde{m}, \tilde{\zeta}$ are still a solution for Equation (1) determined by an innovative spectral issue of Equations (58) and (59). In other words, for solitons, we can generate novel solutions to the existing ones via the gauge transformation. It is crucial to choose a suitable Darboux matrix (\mathcal{T}). By doing this, we develop a certain \mathcal{T} in the following form:

$$\mathcal{T} = \mathcal{T}(\mu) = \begin{pmatrix} \mathcal{T}_{11}(\mu) & \mathcal{T}_{12}(\mu) \\ \mathcal{T}_{21}(\mu) & \mathcal{T}_{22}(\mu) \end{pmatrix} = \begin{pmatrix} \gamma^M + \sum_{i=0}^{M-1} \mathcal{A}^i \gamma^i & \sum_{i=0}^{M-1} \mathcal{B}^i \gamma^i \\ -\sigma \sum_{i=0}^{M-1} \mathcal{B}^{i*} \gamma^i & \gamma^M + \sum_{i=0}^{M-1} \mathcal{A}^{i*} \gamma^i \end{pmatrix}, \tag{62}$$

whereas the complex variables \mathcal{A}^i and \mathcal{B}^i ($i = 0, 1, \dots, M - 1$) are $2M$. When the linear arithmetic problem is solved, it is possible to provide indeterminate functions $\mathcal{T}(\mu)_q \Psi_q(\mu)_q = 0$ ($q = 1, 2, \dots, M$) with $2M$ equations, i.e.,

$$\left[\mu_q^M + \sum_{i=0}^{M-1} \mathcal{A}^i(\mu_q) \mu_q^i \right] \phi_q(\mu_q) + \left[\sum_{i=0}^{M-1} \mathcal{B}^i(\mu_q) \mu_q^i \right] \varphi_q(\mu_q) = 0, \tag{63}$$

$$\left[-\sigma + \sum_{i=0}^{M-1} \mathcal{B}^{i*}(\mu_q) \mu_q^i \right] \phi_q(\mu_q) + \left[\mu_q^M + \sum_{i=0}^{M-1} \mathcal{B}^i(\mu_q) \mu_q^i \right] \varphi_q(\mu_q) = 0,$$

as $\Psi_q(\mu_q) = (\phi_q(\mu_q), \varphi_q(\mu_q))^T = (\phi_q, \varphi_q)^T$ ($q = 1, 2, \dots, M$), which are M solutions for the Lax pairing of Equations (55) and (56) regarding the particular spectrum characteristics μ_q and the original solutions $m_0 = m_0(x, t)$, $\xi_0 = \xi_0(x, t)$, $\mu_q(\mu_q \neq \mu_i, q \neq i, i, q = 1, 2, \dots, M)$, according to the determinant of the equation’s coefficients, have certain diverse parameters that have been chosen appropriately (63).

$$\det \mathcal{T}(\mu) = \prod_{q=1}^M (\mu - \mu_q) (\mu - \mu_q^*). \tag{64}$$

We substitute Equation (62) into Equation (59) with Equation (63).

Theorem 1. Assume $\Psi_1(\mu_1), \Psi_2(\mu_2), \dots, \Psi_M(\mu_M)$ are the responses to M , a varied unit vector addressing the spectral issues for Equations (55) and (56) of the spectrum parameter $\mu_1, \mu_2, \dots, \mu_M$ and the original solution m_0, ξ_0 to Equation (1); then, using the following formulas,

$$\tilde{m}_M = m_0 + 2i\mathcal{B}^{(M-1)}, \quad \tilde{\xi}_M = \xi_0 - i\mathcal{A}_t^{(M-1)}, \tag{65}$$

where $\mathcal{B}^{(M-1)} = \frac{\Delta \mathcal{B}^{(M-1)}}{\Delta_M}$, $\mathcal{A}^{(M-1)} = \frac{\Delta \mathcal{A}^{(M-1)}}{\Delta_M}$ with

$$\Delta_M = \begin{vmatrix} \mu_1^{M-1} \phi_1 & \mu_1^{M-2} \phi_1 & \dots & \phi_1 & \mu_1^{M-1} \phi_1 & \mu_1^{M-2} \phi_1 & \dots & \phi_1 \\ \mu_2^{M-1} \phi_2 & \mu_2^{M-2} \phi_2 & \dots & \phi_2 & \mu_2^{M-1} \phi_2 & \mu_2^{M-2} \phi_2 & \dots & \phi_2 \\ \dots & \dots \\ \mu_M^{M-1} \phi_M & \mu_M^{M-2} \phi_M & \dots & \phi_M & \mu_M^{M-1} \phi_M & \mu_M^{M-2} \phi_M & \dots & \phi_M \\ (\mu_1^{M-1})^* \varphi_1^* & (\mu_1^{M-2})^* \varphi_1^* & \dots & \varphi_1^* & -\sigma^* (\mu_1^{M-1})^* \varphi_1^* & -\sigma^* (\mu_1^{M-2})^* \varphi_1^* & \dots & -\sigma^* \varphi_1^* \\ (\mu_2^{M-1})^* \varphi_2^* & (\mu_2^{M-2})^* \varphi_2^* & \dots & \varphi_2^* & -\sigma^* (\mu_2^{M-1})^* \varphi_2^* & -\sigma^* (\mu_2^{M-2})^* \varphi_2^* & \dots & -\sigma^* \varphi_2^* \\ \dots & \dots \\ (\mu_M^{M-1})^* \varphi_M^* & (\mu_M^{M-2})^* \varphi_M^* & \dots & \varphi_M^* & -\sigma^* (\mu_M^{M-1})^* \varphi_M^* & -\sigma^* (\mu_M^{M-2})^* \varphi_M^* & \dots & -\sigma^* \varphi_M^* \end{vmatrix},$$

while $\Delta \mathcal{A}^{(M-1)}$ and $\Delta \mathcal{B}^{(M-1)}$ are expressed through the determinant Δ_M by replacing its first and $(M + 1)$ -th columns with the column vector $(-\mu_1^M \phi_1, \dots, -\mu_M^M \phi_M, -(\mu_1^M)^* \varphi_1^*, -(\mu_2^M)^* \varphi_2^*, \dots, -(\varphi_M^M)^* \varphi_M^*)^T$, respectively.

The N -fold DT of Equation (1) is transformed to Equations (57) and (65) using the spectrum variables M and μ_q . Theorem 1’s proof is provided by simple calculation; the readers are left with the task of determining the specifics of the proof’s procedure in light of the fact that they can consult the pertinent literature [27] for further information.

3.2. Asymptotic State Analysis and Solutions to Bright–Dark Multi-Soliton Systems

By utilizing the DT obtained in the preceding part, we can generate solitons on a constant background of Equation (1). In order to produce a single fundamental solution with $\mu = \mu_q$ as shown below, we first take the initial solutions $m_0 = 0$ and $\xi_0 = 1$ as the constant solution.

$$\Psi_q = \begin{pmatrix} \phi_q \\ \varphi_q \end{pmatrix} = \begin{pmatrix} e^{\frac{i(-\mu_q^2 x - \mu_q \gamma x + t)}{\mu_q + \gamma}} \\ e^{\frac{-i(-\mu_q^2 x - \mu_q \gamma x + t)}{\mu_q + \gamma}} \end{pmatrix}. \tag{66}$$

The following always uses the parameters $\gamma = \sigma = 1$ to conveniently gain the dynamic properties of soliton solutions. The M -soliton solutions of Equation (1) can therefore be obtained from Equation (65). We depict their structures as seen in Figures 1–13 to better comprehend their physical characteristics and interactions in Figures 14–16 when $M = 1, 2, 3, 4$.

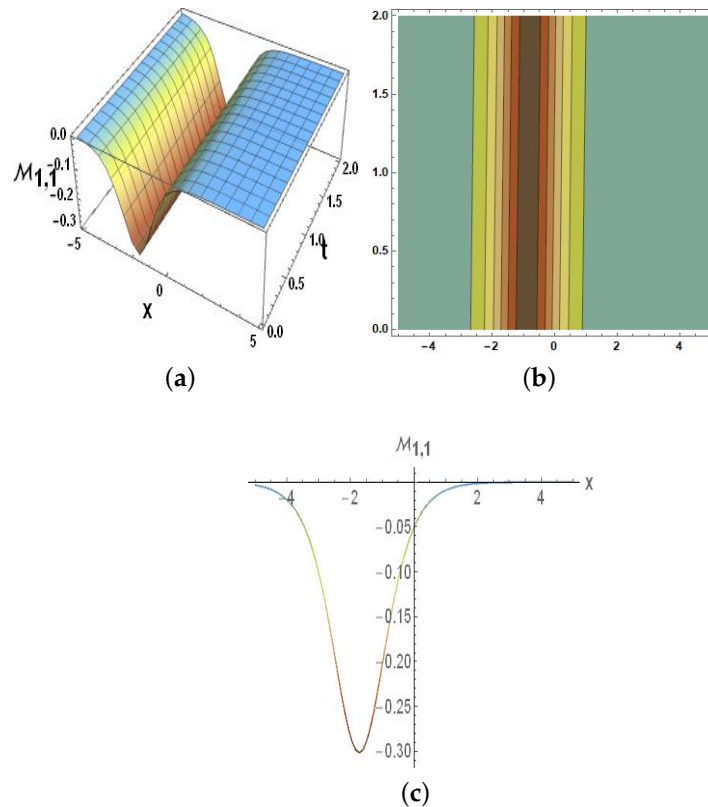


Figure 1. The parametric values $\mathcal{L} = 0.5$, $f_0 = 0.2$, $m = 0.3$, and $s_2 = 0.1$ display the graphical representation of $M_{1,1}$ in Equation (34). (a) Three dimensions at $y = 2$, $z = 0.3$. (b) Contour at $y = 2$, $z = 0.3$. (c) Two dimensions at $y = 2$, $z = 0.3$, $t = 1$.

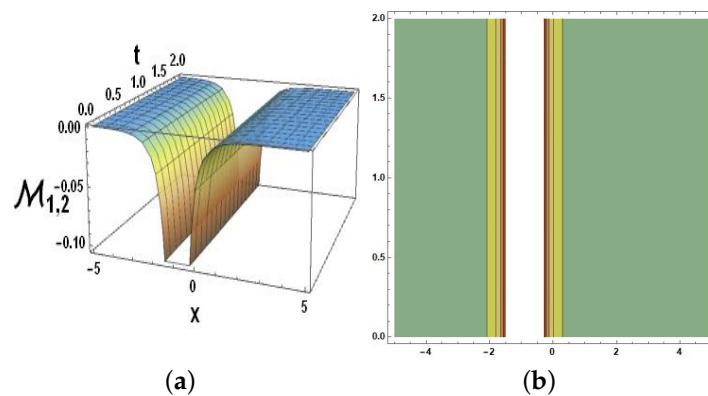


Figure 2. Cont.

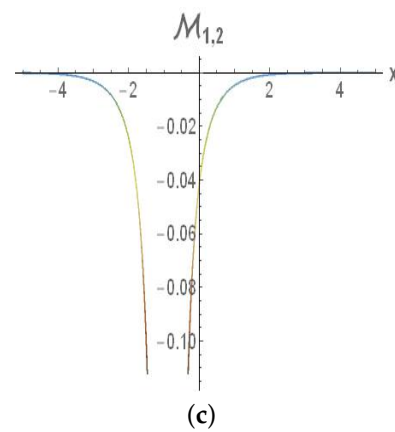


Figure 2. The parametric values $\mathcal{L} = 0.15$, $f_0 = 0.5$, $m = 0.3$, and $s_2 = 1.1$ display the graphical representation of $\mathcal{M}_{1,2}$ in Equation (35). (a) Three dimensions at $y = 1$, $z = 0.3$. (b) Contour at $y = 1$, $z = 0.3$. (c) Two dimensions at $y = 1$, $z = 0.3$, $t = 1$.

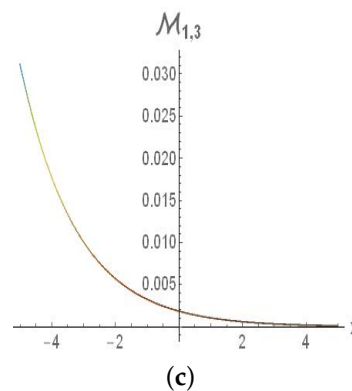
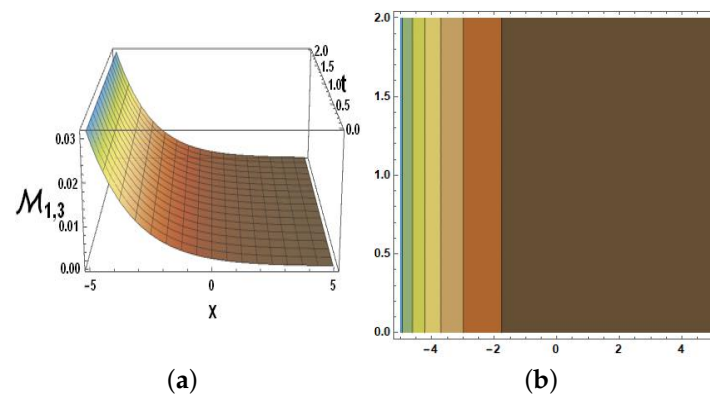


Figure 3. The parametric values $\mathcal{L} = 0.9$, $f_0 = 0.8$, $m = 1.3$, and $s_2 = 0.9$ display the graphical representation of $\mathcal{M}_{1,3}$ in Equation (36). (a) Three dimensions at $y = 1.6$, $z = 0.5$. (b) Contour at $y = 1.6$, $z = 0.5$. (c) Two dimensions at $y = 1.6$, $z = 0.5$, $t = 1$.

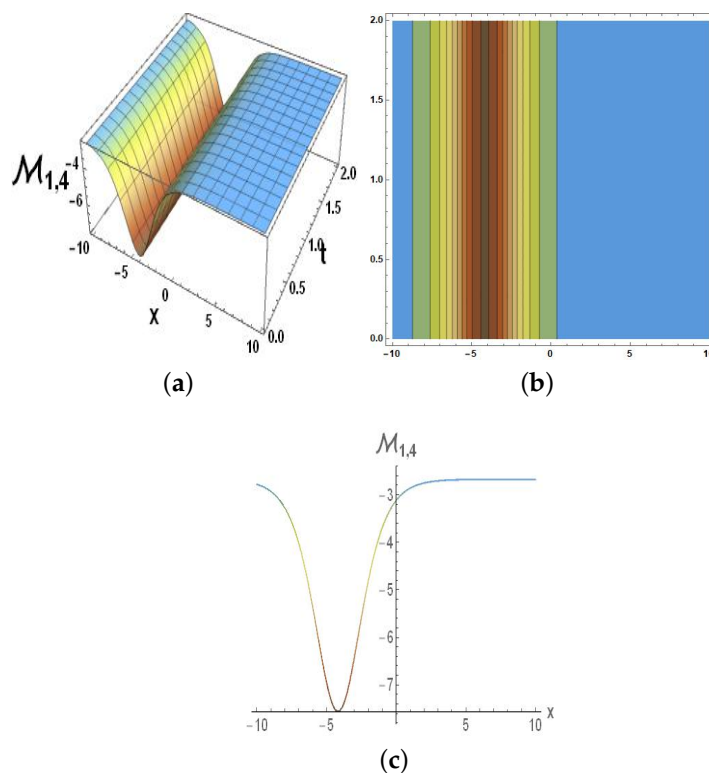


Figure 4. The parametric values $\mathcal{L} = 1.5$, $f_0 = 0.3$, $m = 0.3$, and $s_2 = 0.4$ display the graphical representation of $M_{1,4}$ in Equation (37). (a) Three dimensions at $y = 3.1$, $z = 1.3$. (b) Contour at $y = 3.1$, $z = 1.3$. (c) Two dimensions at $y = 3.1$, $z = 1.3$, $t = 1$.

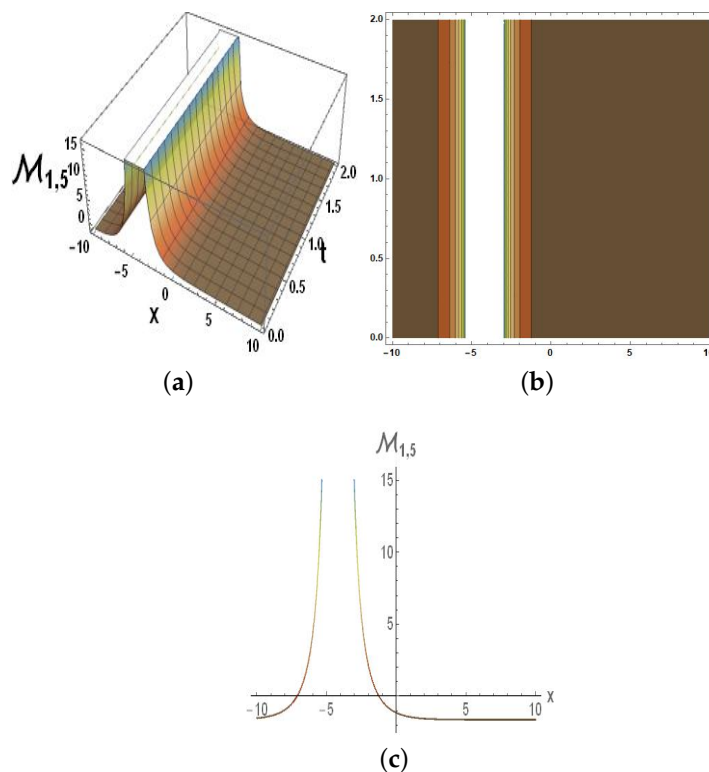


Figure 5. The parametric values $\mathcal{L} = 0.7$, $f_0 = 1.2$, $m = 0.3$, and $s_2 = 1.1$ display the graphical representation of the $S_{1,5}$ in Equation (38). (a) Three dimensions at $y = 3.1$, $z = 1.3$. (b) Contour at $y = 3.1$, $z = 1.3$. (c) Two dimensions at $y = 3.1$, $z = 1.3$, $t = 1$.

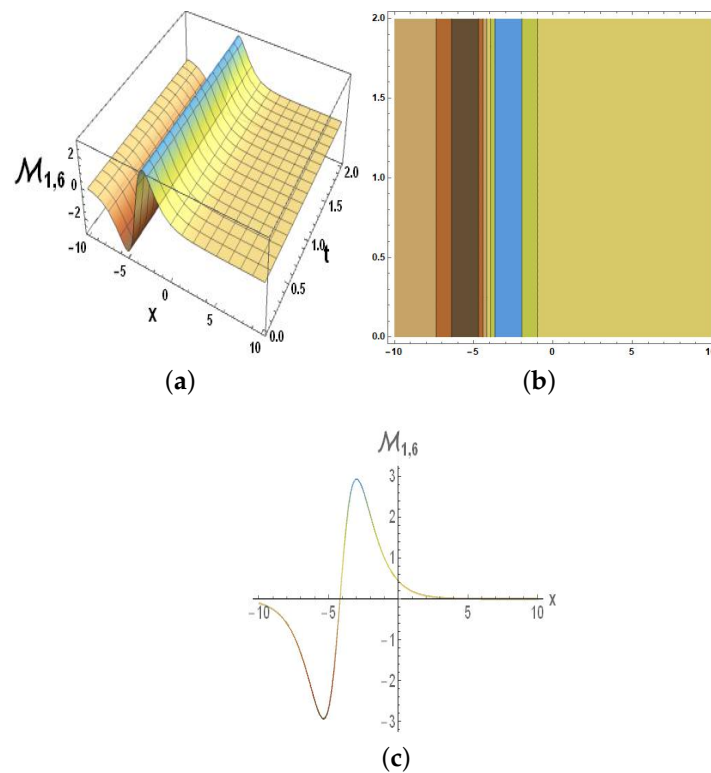


Figure 6. The parametric values $\mathcal{L} = 1$, $f_0 = 1.2$, $m = 0.8$, and $s_2 = 0.2$ display the graphical representation of $M_{1,6}$ in Equation (39). (a) Three dimensions at $y = 2$, $z = 0.3$. (b) Contour at $y = 2$, $z = 0.3$. (c) Two dimensions at $y = 2$, $z = 0.3, t = 1$.

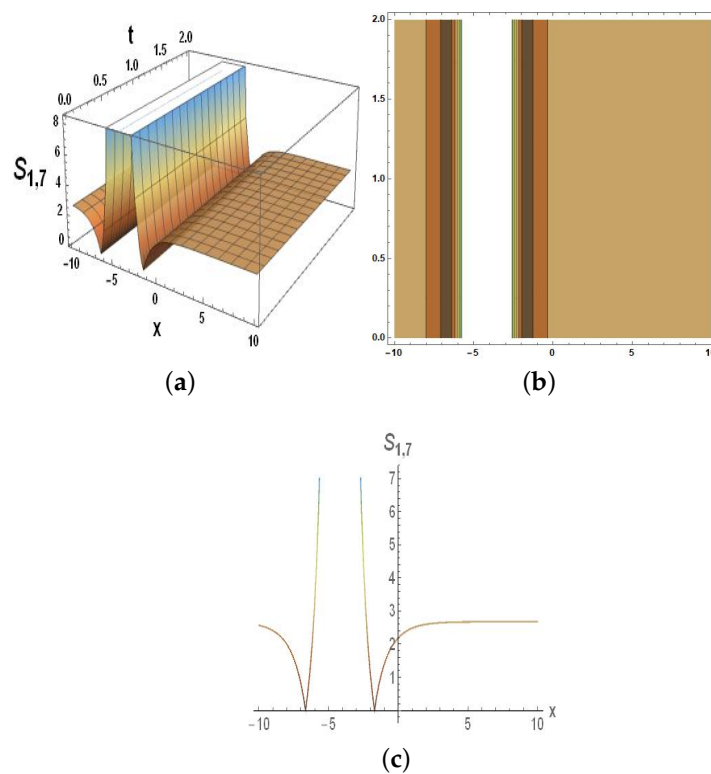


Figure 7. The parametric values $\mathcal{L} = 2.5$, $f_0 = 1.2$, $m = 0.4$, and $s_2 = 0.8$ display the graphical representation of the $M_{1,7}$ in Equation (40). (a) Three dimensions at $y = 1$, $z = 1.3$. (b) Contour at $y = 1$, $z = 1.3$. (c) Two dimensions at $y = 1$, $z = 1.3, t = 1$.

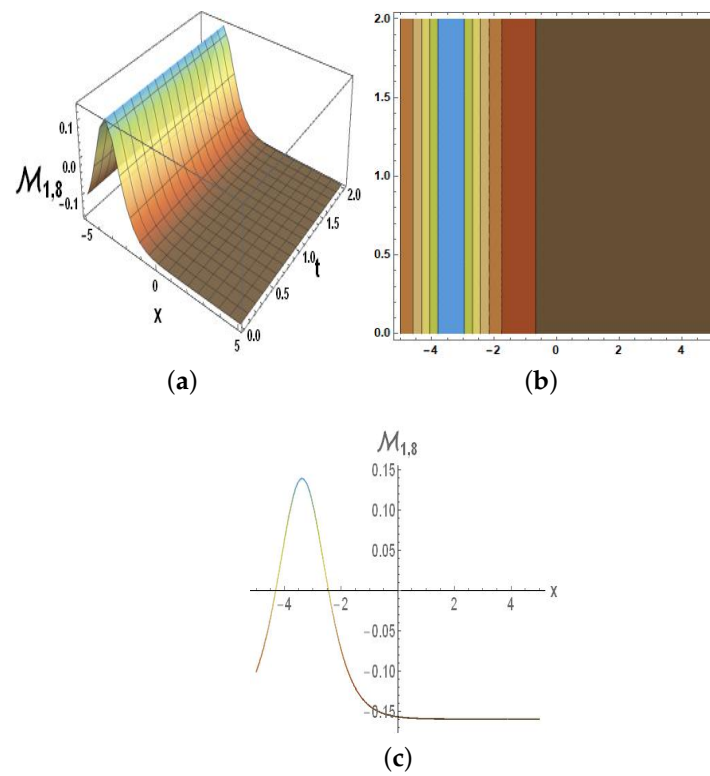


Figure 8. The parametric values $\mathcal{L} = 0.5$, $f_0 = 0.2$, $m = 0.3$, $y = 2$, $z = 0.3$, and $s_2 = 0.1$ display the graphical representation of $M_{1,8}$ in Equation (41). (a) Three dimensions at $y = 2$, $z = 0.3$. (b) Contour at $y = 2$, $z = 0.3$. (c) Two dimensions at $y = 2$, $z = 0.3$, $t = 1$.

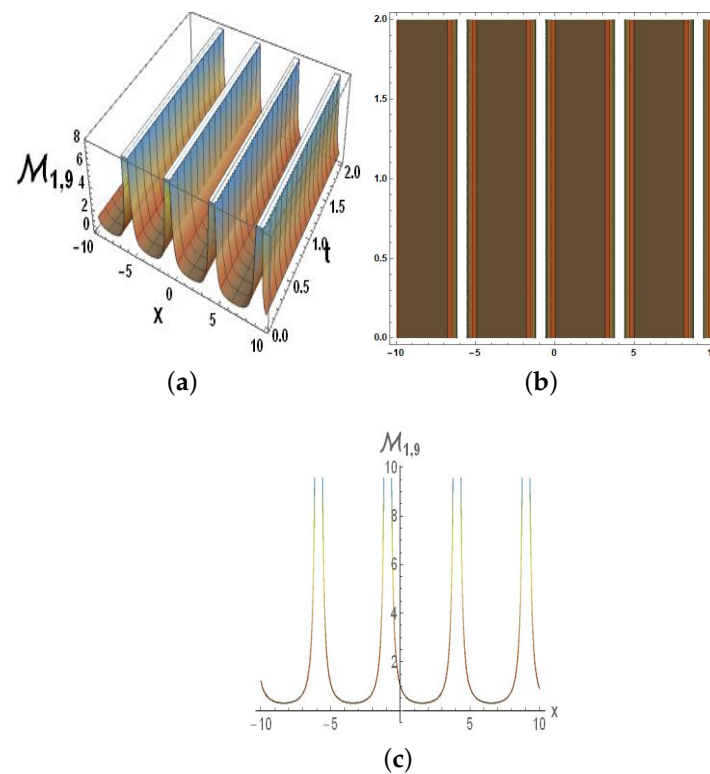


Figure 9. The parametric values $\mathcal{L} = 0.66$, $f_0 = 0.112$, $m = 0.3$, and $s_2 = 0.56$ display the graphical representation of $M_{1,9}$ in Equation (42). (a) Three dimensions at $y = 2$, $z = 0.43$. (b) Contour at $y = 2$, $z = 0.43$. (c) Two dimensions at $y = 2$, $z = 0.43$, $t = 1$.

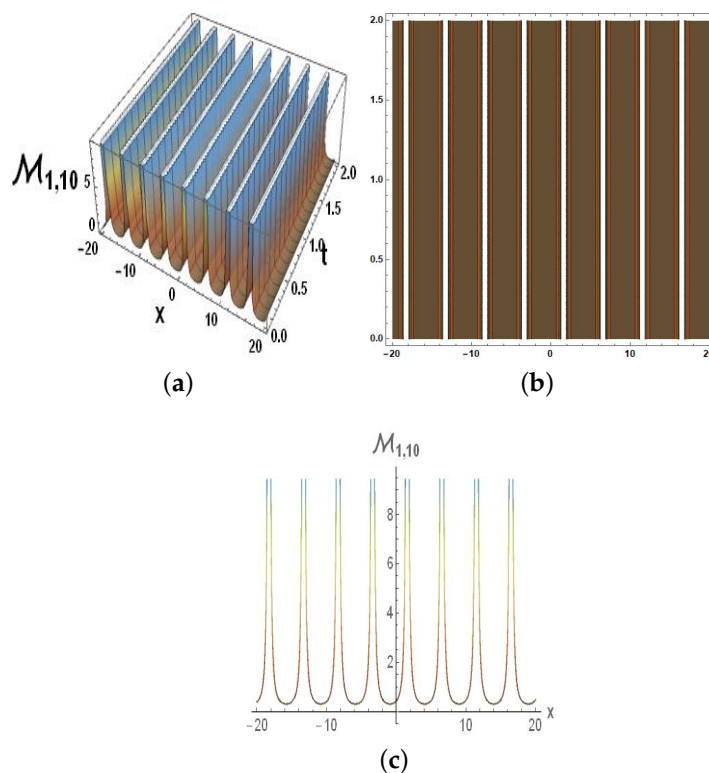


Figure 10. The parametric values $\mathcal{L} = 0.55$, $f_0 = 0.12$, $m = 0.3$, and $s_2 = 0.71$ display the graphical representation of $M_{1,10}$ in Equation (43). (a) Three dimensions at $y = 2$, $z = 0.63$. (b) Contour at $y = 2$, $z = 0.63$. (c) Two dimensions at $y = 2$, $z = 0.63$, $t = 1$.

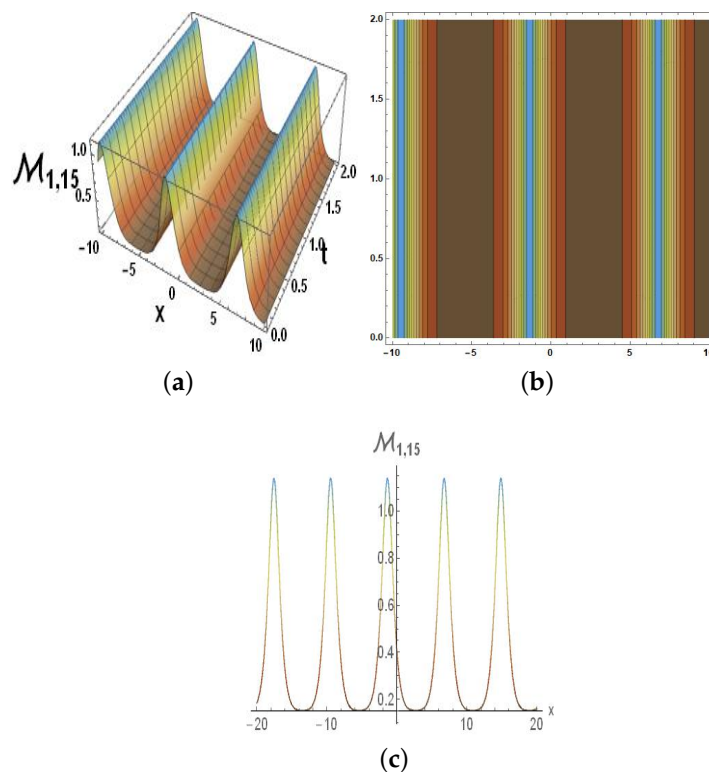


Figure 11. The parametric values $\mathcal{L} = 0.25$, $f_0 = 0.42$, $m = 0.3$, and $s_2 = 0.71$ display the graphical representation of $S_{1,15}$ in Equation (48). (a) Three dimensions at $y = 1.2$, $z = 0.63$. (b) Contour at $y = 1.2$, $z = 0.63$. (c) Two dimensions at $y = 1.2$, $z = 0.63$, $t = 1$.

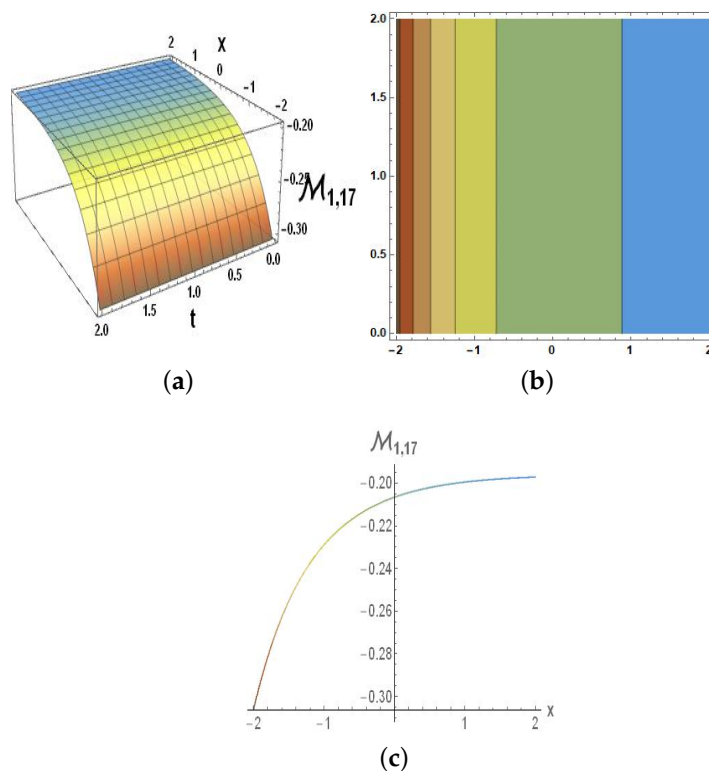


Figure 12. The parametric values $\mathcal{L} = 0.75$, $f_0 = 0.2$, $m = 0.3$, and $s_2 = 0.1$ display the graphical representation of $M_{1,17}$ in Equation (50). (a) Three dimensions at $y = 1$, $z = 0.3$. (b) Contour at $y = 1$, $z = 0.3$. (c) Two dimensions at $y = 1$, $z = 0.3, t = 1$.

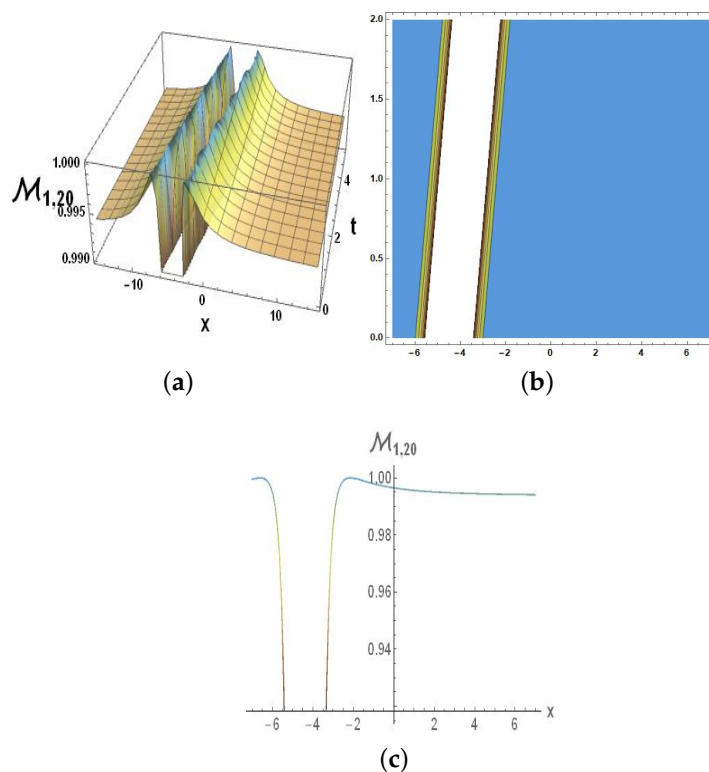


Figure 13. The parametric values $\mathcal{L} = 0.5$, $f_0 = 0.5$, $m = 0.3$, and $s_2 = 0.4$ display the graphical representation of $M_{1,20}$ in Equation (53). (a) Three dimensions at $y = 2$, $z = 0.3$. (b) Contour at $y = 2$, $z = 0.3$. (c) Two dimensions at $y = 2$, $z = 0.3, t = 1$.

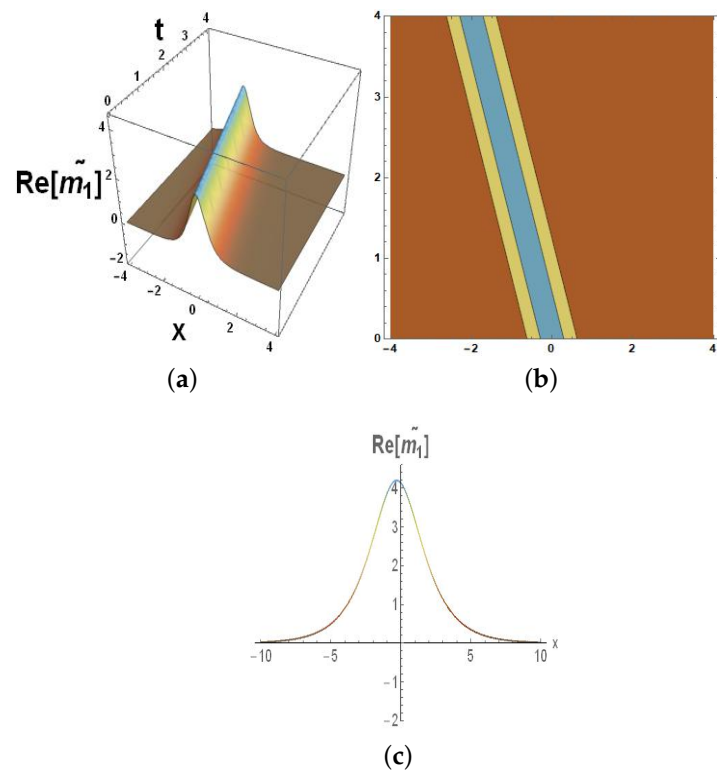


Figure 14. The parametric values $\mathcal{L} = 0.5$, $f_0 = 0.2$, $m = 0.3$, and $s_2 = 0.1$ display the graphical representation of $Re[\tilde{m}_1]$ in Equation (68). (a) Three dimensions at $y = 2$, $z = 0.3$. (b) Contour at $y = 2$, $z = 0.3$. (c) Two dimensions at $y = 2$, $z = 0.3, t = 1$.

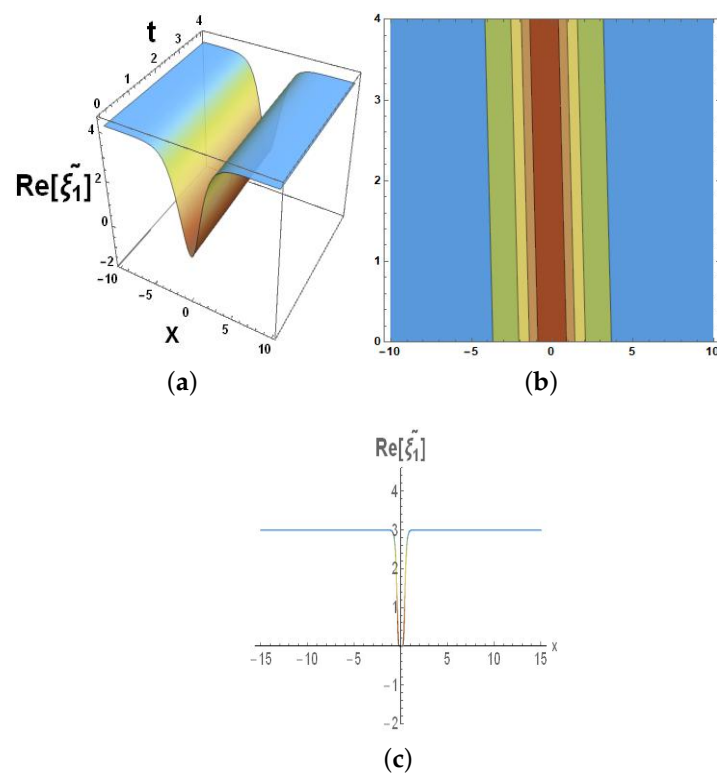


Figure 15. The parametric values $\mathcal{L} = 0.5$, $f_0 = 0.2$, $m = 0.3$, and $s_2 = 0.1$ display the graphical representation of $Re[\tilde{\xi}_1]$ in Equation (68). (a) Three dimensions at $y = 2$, $z = 0.3$. (b) Contour at $y = 2$, $z = 0.3$. (c) Two dimensions at $y = 2$, $z = 0.3, t = 1$.

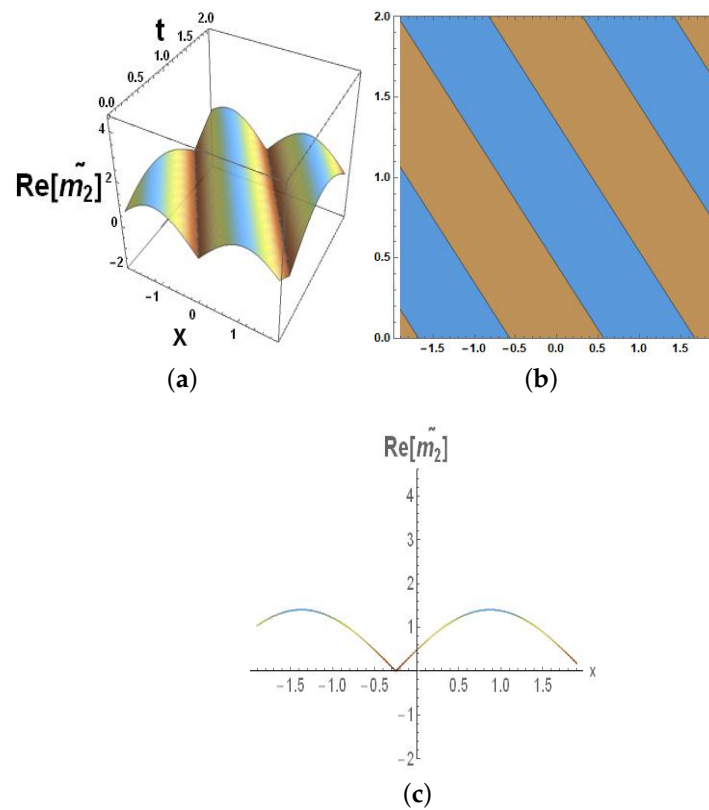


Figure 16. The parametric values $\mathcal{L} = 0.5$, $f_0 = 0.2$, $m = 0.3$, and $s_2 = 0.1$, display the graphical representation of $\text{Re}[\tilde{m}_2]$ in Equation (71). (a) Three dimensions at $y = 2$, $z = 0.3$. (b) Contour at $y = 2$, $z = 0.3$. (c) Two dimensions at $y = 2$, $z = 0.3$, $t = 1$.

3.2.1. Dynamic Analysis and One-Soliton Solutions

For $M = 1$, $\mu_1 = c + di$, where c and d are constant, from Theorem 1, we obtain the solution

$$\tilde{m}_1 = 2i \frac{\Delta \mathcal{B}^{(0)}}{\Delta_1}, \quad \tilde{\zeta}_1 = 1 - i \left(\frac{\Delta \mathcal{A}^{(0)}}{\Delta_1} \right)_t \tag{67}$$

where

$$\Delta_1 = \begin{vmatrix} \phi_1 & \varphi_1 \\ \varphi_1^* & -\sigma^* \phi_1^* \end{vmatrix}, \Delta \mathcal{A}^{(0)} = \begin{vmatrix} -\mu_1 \phi_1 & \varphi_1 \\ -\mu_1^* \varphi_1^* & -\sigma^* \phi_1^* \end{vmatrix}, \Delta \mathcal{B}^{(0)} = \begin{vmatrix} \phi_1 & -\mu_1 \phi_1 \\ \varphi_1^* & -\mu_1^* \varphi_1^* \end{vmatrix}.$$

We convert the responses to their equations to examine their physical characteristics in Equation (67) as

$$\tilde{m}_1 = 2de^{2i\zeta_{Im}} \text{sech}(2\zeta_{Re}), \quad \tilde{\zeta}_1 = 1 - \frac{2d^2}{q} \text{sech}^2(2\zeta_{Re}), \tag{68}$$

as $\zeta_{Re} = \left(dx + \frac{d}{q}t\right)$, $\zeta_{Im} = \left[-cx + (c + 1)\frac{t}{q}\right]$, with $q = c^2 + d^2 + 2c + 1$.

It is simple to observe that \tilde{m}_1 is a bright soliton framework, and $\tilde{\zeta}_1$ is a dark soliton, from the solutions to Equation (68), and the physical characteristics, such as the intensity, dimension, speed, wave numbers, main phase, and energy, which are listed in Table 1, can also be easily probed. For m_1 and ζ_1 , the energies are defined as $F_{m_1} = \int_{-\infty}^{\infty} |m_1|^2 dx$, $F_{\zeta_1} = \int_{-\infty}^{\infty} (\zeta_1 - 1)^2 dx$. We can easily observe the amplitudes and velocities of one-soliton solutions depending on the spectral parameter μ_1 . Figures 15 and 16 show the bell-shaped bright one-soliton structure of \tilde{m}_1 and the anti-bell-shaped dark one-soliton structure of $\tilde{\zeta}_1$, when $\mu_1 = 1 + 2i$ (i.e., $c = 1, d = 2$).

Table 1. The one-soliton solutions’ physical characteristics.

Solitons	Intensity	Dimensions	Speed	Wave Numbers	Main Phases	Energies
\tilde{m}_1	$2c$	$\frac{1}{2c}$	$-\frac{1}{q}$	$2c$	0	$4c$
$\tilde{\zeta}_1 - 1$	$\frac{2c^2}{q}$	$\frac{1}{2c}$	$-\frac{1}{q}$	$2c$	0	$\frac{8c^3}{3q^2}$

3.2.2. Analysis of Two-Soliton Solutions Asymptotically

When $M = 2, \mu_1 = c_1 + d_1i, \mu_2 = c_2 + d_2i$, where c_1, c_2, d_1, d_2 , according to Theorem 1, are positive independent variables, and twofold DT can provide the following:

$$\tilde{m}_2 = 2i \frac{\mathcal{A}\mathcal{B}^{(i)}}{\mathcal{A}_2}, \quad \tilde{\zeta}_2 = 1 - i \left(\frac{\mathcal{A}\mathcal{A}^{(1)}}{\mathcal{A}_2} \right), \tag{69}$$

where

$$\tilde{m}_2 = \frac{n_1 e^{\tilde{\zeta}_2^*} + n_2 e^{\tilde{\zeta}_1^* + \tilde{\zeta}_2 + \tilde{\zeta}_2^*} + n_2^* e^{\tilde{\zeta}_1^*} + n_1^* e^{\tilde{\zeta}_1 + \tilde{\zeta}_1^* + \tilde{\zeta}_2}}{n_3 (e^{\tilde{\zeta}_1^* + \tilde{\zeta}_2} + e^{\tilde{\zeta}_1 + \tilde{\zeta}_2^*}) + n_4 (1 + e^{\tilde{\zeta}_1 + \tilde{\zeta}_1^* + \tilde{\zeta}_2 + \tilde{\zeta}_2^*}) + n_5 (e^{\tilde{\zeta}_1 + \tilde{\zeta}_1^*} + e^{\tilde{\zeta}_2 + \tilde{\zeta}_2^*})}, \quad \tilde{\zeta}_2 = \frac{G_1}{G_2}, \tag{70}$$

where

$$G_1 = W_1 \cosh(\zeta_1^* - \zeta_2^*) + W_2 \cosh(\zeta_1 + \zeta_2^*) + W_2^* \cosh(\zeta_1^* + \zeta_2) + W_1^* \cosh(\zeta_1 - \zeta_2) + W_3 \cosh[(\zeta_2 - \zeta_2^*) - (\zeta_1 - \zeta_1^*)] + W_4 \cosh(\zeta_1 + \zeta_1^* + \zeta_2 + \zeta_2^*) + W_5 \cosh(\zeta_2 + \zeta_2^*) + W_6 \cosh[\zeta_1 + \zeta_1^* - (\zeta_2 + \zeta_2^*)] + W_7 + W_8 \cosh(\zeta_1 + \zeta_1^*),$$

$$G_2 = 2q_1 q_2 \left[W_9 \cosh\left(\frac{\zeta_1 - \zeta_1^* - (\zeta_2 - \zeta_2^*)}{2}\right) + W_{10} \cosh\left(\frac{\zeta_1 + \zeta_1^* + \zeta_2 + \zeta_2^*}{2}\right) + W_{11} \cosh\left(\frac{\zeta_1 + \zeta_1^* - (\zeta_2 + \zeta_2^*)}{2}\right) \right]^2,$$

with

$$\zeta_1 = 2(d_1 + c_1i)x + \frac{2(d_1 - c_1i - i)}{q_1}t,$$

$$\zeta_2 = -2(d_2 - c_2i)x - \frac{2(d_2 - c_2i - i)}{q_2}t,$$

$$q_1 = c_1^2 + d_1^2 + 2c_1 + 1,$$

$$q_2 = c_2^2 + d_2^2 + 2c_2 + 1,$$

$$n_1 = [4d_2(c_1 - c_2)^2 + 4d_2^3 - 4d_1^2d_2] - 8d_1d_2(c_1 - c_2)i,$$

$$n_2 = [4d_1(c_1 - c_2)^2 + 4d_1^3 - 4d_1d_2^2] - 8d_1d_2(c_2 - c_1)i^2,$$

$$n_3 = W_9 = -4d_1d_2,$$

$$n_4 = W_{10} = (c_1 - c_2)^2 + (d_1 + d_2)^2,$$

$$n_5 = W_{11} = (c_1 - c_2)^2 + (d_1 - d_2)^2,$$

$$W_1 = [-8d_1d_2n_5(c_1^3c_2 - c_1^2c_2^2 - c_1^2d_1d_2 - c_1^2d_2^2 + c_1c_2^3 + c_1c_2d_1^2 + c_1c_2d_2^2 - c_2^2d_1^2 - c_2^2d_1d_2 - d_1^3d_2 - d_1^2d_2^2 - d_1d_2^3 + c_1^3 + c_1^2c_2 + c_1c_2^2 + c_1d_1^2 - 2c_1d_1d_2 - c_1d_2^2 + c_2^3 - c_2d_1^2 - 2c_2d_1d_2 + c_2d_2^2 + 2c_1^2 + 2c_1c_2 + 2c_2^2 - 2d_1c_2 + 2c_1 + 2c_2 + 1)] + 8d_1d_2n_5(c_1d_2 + c_2d_1 + d_1 + d_2)(c_1^2 - c_2^2 + d_1^2 - d_2^2 + 2c_1 - 2c_2)i,$$

$$W_2 = [-8d_1d_2n_4(c_1^3c_2 - c_1^2c_2^2 + c_1^2d_1d_2 - c_1^2d_2^2 + c_1c_2^3 + c_1c_2d_1^2 + c_1c_2d_2^2 - c_2^2d_1^2 + c_2^2d_1d_2 + d_1^3d_2 - d_1^2d_2^2 + d_1d_2^3 + c_1^3 + c_1^2c_2 + c_1c_2^2 + c_1d_1^2 + 2c_1d_1d_2 - c_1d_2^2 + c_2^3 - c_2d_1^2 + 2c_2d_1d_2 + c_2d_2^2 + 2c_1^2 + 2c_1c_2 + 2c_2^2 + 2d_1d_2 + 2c_1 + 2c_2 + 1)] + 8d_1d_2n_4(c_1d_2 - c_2d_1 - d_1 + d_2)(c_1^2 - c_2^2 + d_1^2 - d_2^2 + 2c_1 - 2c_2)i,$$

$$\begin{aligned}
W_3 &= d_1^2 d_2^2 [16(c_1 + 1)^2 + 16d_1^2] [(c_2 + 1)^2 + d_2^2], \\
W_4 &= n_4^2 [(c_1 + 1)^2 + d_1^2] [(c_2 + 1)^2 + d_2^2], \\
W_5 &= 2n_4 n_5 [-3d_1^2 + (c_1 + 1)^2] [(c_2 + 1)^2 + d_2^2], \\
W_6 &= n_5^2 [(c_1 + 1)^2 + d_1^2] [(c_2 + 1)^2 + d_2^2], \\
W_7 &= [36d_2^2 - 12(c_2 + 1)^2] d_1^6 + \left\{ -8d_2^4 + [60c_1^2 + (112c_2 + 232)c_1 - 96c_2^2 - 80c_2 + 76] d_2^2 - 20[c_1^2 - (2.4c_2 \right. \\
&\quad \left. + 0.4)c_1 + 1.2c_2^2 - 0.2] (c_2 + 1)^2 \right\} d_1^4 + \left\{ 36d_2^6 + [-96c_1^2 + (112c_2 - 80)c_1 + 60c_2^2 + 232c_2 + 76] d_2^4 \right. \\
&\quad \left. + [12c_1^4 + (160c_2 + 208)c_1^3 + (-288c_2^2 - 96c_2 + 264)c_1^2 + (160c_2^3 - 96c_2^2 - 192c_2 + 112)c_1 + 12c_2^4 \right. \\
&\quad \left. + 208c_2^3 + 264c_2^2 + 112c_2 + 56] d_2^2 - 4(c_1 - c_2)^2 (c_2 + 1)^2 [c_1^2 + (-6c_2 - 4)c_1 + 3c_2^2 - 2] \right\} d_1^2 + 4[d_2^2 \\
&\quad \left. + (c_1 - c_2)^2 \right]^2 [-3d_2^2 + (c_2 + 1)^2] (c_1 + 1)^2, \\
W_8 &= 2n_4 n_5 [(c_1 + 1)^2 + d_1^2] [-3d_2^2 + (c_2 + 1)^2].
\end{aligned}$$

The expression of Equation (68) is a solution with two solitons. The distinctive feature of an elastic collision is that system's total energy is unaffected by the collision either before or after it occurs. To determine that whenever two objects collide, the solitons are elastic, the asymptotic of the soliton collision is a very effective technique. These are the two states of the two solitons at zero and infinity. We correlate these to the two temporal patterns that we depict in the propagation process. Of course, we can also speculate about the particular set of parameters $c_1 > 0, c_2 > 0, d_1 < 0, d_2 < 0$. The examination of the asymptotic states for possibilities of Equation (68) obtains the following eight asymptotic expressions.

(i) With regard to this aspect \tilde{m}_2 in the addresses for Equation (68):
Before the collision ($t \rightarrow -\infty$),

$$\begin{aligned}
\tilde{m}_1 \rightarrow \epsilon_1^- &= \frac{n_2^*}{2\sqrt{n_4 n_5}} e^{-\zeta_{1Im} i} \operatorname{sech} \left(\zeta_{1Re} - \frac{1}{2} \ln \frac{n_4}{n_5} \right), \quad (\zeta_1 + \zeta_1^* \sim 0, \quad \zeta_2 + \zeta_2^* \rightarrow -\infty), \\
\tilde{m}_1 \rightarrow \epsilon_2^- &= \frac{n_1^*}{2\sqrt{n_4 n_5}} e^{-\zeta_{2Im} i} \operatorname{sech} \left(\zeta_{2Re} + \frac{1}{2} \ln \frac{n_4}{n_5} \right), \quad (\zeta_2 + \zeta_2^* \sim 0, \quad \zeta_1 + \zeta_1^* \rightarrow +\infty),
\end{aligned} \tag{71}$$

where ϵ_1^- and ϵ_2^- are asymptotic illustrations of \tilde{m}_2 before they smash into one another.
After a collision ($t \rightarrow +\infty$),

$$\begin{aligned}
\tilde{m}_2 \rightarrow \epsilon_1^+ &= \frac{n_2}{2\sqrt{n_4 n_5}} e^{-\zeta_{1Im} i} \operatorname{sech} \left(\zeta_{1Re} + \frac{1}{2} \ln \frac{n_4}{n_5} \right), \quad (\zeta_1 + \zeta_1^* \sim 0, \quad \zeta_2 + \zeta_2^* \rightarrow +\infty), \\
\tilde{m}_2 \rightarrow \epsilon_2^+ &= \frac{n_1}{2\sqrt{n_4 n_5}} e^{-\zeta_{2Im} i} \operatorname{sech} \left(\zeta_{2Re} - \frac{1}{2} \ln \frac{n_4}{n_5} \right), \quad (\zeta_2 + \zeta_2^* \sim 0, \quad \zeta_1 + \zeta_1^* \rightarrow -\infty),
\end{aligned} \tag{72}$$

where ϵ_1^+ and ϵ_2^+ are the formulas of \tilde{m}_2 that asymptotically follow their collision. When assessed by Equations (71) and (72), through direct calculation, we can obtain

(ii) With regard to the element $\tilde{\xi}_2$ as solution to Equation (68):
Before the collision ($t \rightarrow -\infty$),

$$\begin{aligned}
\tilde{\xi}_1 - 1 \rightarrow \tau_1^- &= -\frac{2d_1^2}{q_1} \operatorname{sech}^2 \left(\zeta_{1Re} - \frac{1}{2} \ln \frac{W_{10}}{W_{11}} \right), \quad (\zeta_1 + \zeta_1^* \sim 0, \quad \zeta_2 + \zeta_2^* \rightarrow -\infty), \\
\tilde{\xi}_1 - 1 \rightarrow \tau_2^- &= -\frac{2d_2^2}{q_2} \operatorname{sech}^2 \left(\zeta_{2Re} + \frac{1}{2} \ln \frac{W_{10}}{W_{11}} \right), \quad (\zeta_2 + \zeta_2^* \sim 0, \quad \zeta_1 + \zeta_1^* \rightarrow +\infty),
\end{aligned} \tag{73}$$

where τ_1^- and τ_2^- , prior to their collision with one another, constitute the asymptotic interpretations of $\tilde{\zeta}_2 - 1$.

After a collision ($t \rightarrow +\infty$),

$$\begin{aligned}\tilde{\zeta}_2 - 1 \rightarrow \tau_1^+ &= -\frac{2d_1^2}{q_1} \operatorname{sech}^2\left(\zeta_{1Re} + \frac{1}{2} \ln \frac{W_{10}}{W_{11}}\right), & (\zeta_1 + \zeta_1^* \sim 0, \quad \zeta_2 + \zeta_2^* \rightarrow +\infty), \\ \tilde{\zeta}_2 - 1 \rightarrow \tau_2^+ &= -\frac{2d_1^2}{q_1} \operatorname{sech}^2\left(\zeta_{1Re} - \frac{1}{2} \ln \frac{W_{10}}{W_{11}}\right), & (\zeta_2 + \zeta_2^* \sim 0, \quad \zeta_1 + \zeta_1^* \rightarrow -\infty),\end{aligned}\quad (74)$$

where τ_1^+, τ_2^+ represent the exponential formulations of $\tilde{\zeta}_2 - 1$ following their collision. We deduce the respective physical characteristics of $\tilde{\zeta}_2 - 1$, as shown in Table 2, from the analysis above.

Table 2. Specifications regarding the two-soliton solution's physical state \tilde{m}_2 .

Soliton	Amplitude	Width	Velocity	Wave Numbers	Primary Phase	Energy
ϵ_1^-	$2d_1$	$\frac{1}{2d_1}$	$-\frac{1}{q_1}$	$2d_1$	$\frac{1}{2} \ln \frac{n_4}{n_4}$	$4d_1$
ϵ_2^-	$2d_2$	$\frac{1}{2d_2}$	$-\frac{1}{q_2}$	$2d_2$	$-\frac{1}{2} \ln \frac{n_3}{n_4}$	$4d_2$
ϵ_1^+	$2d_1$	$\frac{1}{2d_1}$	$-\frac{1}{q_1}$	$2d_1$	$-\frac{1}{2} \ln \frac{n_s}{n_s}$	$4d_1$
ϵ_2^+	$2d_2$	$\frac{1}{2d_2}$	$-\frac{1}{q_2}$	$2d_2$	$\frac{1}{2} \ln \frac{n_4}{n_4}$	$4d_2$

In view of the aforementioned discussion, we may conclude that the transmission and impact of two solitons possess the following attributes.

(i) The solitons' amplitudes, lengths, velocity, pulse numbers, formats, and energy are unaffected by the collision in both the before and after states.

(ii) Only the stages of the two solitons that collided have changed, and they are now opposite. As a result, we conclude that the collisions of two solitons become elastic. For a solution to Equation (68), with the parameters $\gamma_1 = 2i$ and $\gamma_2 = i$, Figure 16 shows the significant two-soliton configurations of m_2 and $\tilde{\zeta}_2$. From this, we can see that part \tilde{m}_2 is an exceptional two-soliton framework, while part $\tilde{\zeta}_2$ is a dark two-soliton framework.

4. Results and Discussion

This section covers the comparison of the new work to previous work. Wazwaz et al. [31], studied the (3+1)-dimensional Kadomtsev–Petviashvili equation to find multiple solutions. We compared the innovative soliton solution produced by employing the Sardar substitution and Darboux transformation methods with the preceding article's analysis of the (3+1)-dimensional Kadomtsev–Petviashvili (KP) equation determined using the streamlined Hirota's direct method. The soliton solution that was found in the present research is different from the multiple-soliton solutions that Hirota's direct technique yielded. The solutions of this study have potential applications in a variety of domains, including nonlinear optics, engineering, applied sciences, and communications. These solutions also expand our understanding of nonlinear phenomena. Furthermore, the KP model can be solved using a variety of solutions, and the suggested method's robustness is demonstrated by the consistency and correctness of the results.

This study was used to investigate the (3+1)-dimensional KP model using two different useful techniques, including the MSST and the DT. The aim was to obtain one and two bright and dark soliton solutions and multiple solitary wave solutions.

The studies show that any of the two approaches can be used to successfully arrive at the intended results. Solutions for hyperbolic, trigonometric, singular, dark, and bright solitons were found using the MSST. Then, two bright and two dark solitons were created using the DT. The solutions' physical characteristics were reviewed, and the outcomes were shown using 3-D plots, contour plots, and 2-D curves. The study shows that the

obtained solutions are reliable and may be applied to many physical phenomena in various scientific domains. In conclusion, the study illuminates the behavior of the KP model in (3+1)-dimensional space and emphasizes the efficiency of the MSST and DT in obtaining various soliton solutions. Future research in mathematical physics, engineering, and applied mathematics may be affected by the findings.

We were able to solve Equation (34)–(53) using the MSST, and the results are provided in Figures 1–13, which show the dark, singular, bright, exponential, and periodic solutions as well as their 3-D, 2-D, and contour plot representations.

We were able to solve Equations (67)–(74) using the DT, and the results are shown in Figures 14 and 15, which represent the one-soliton dark and bright solutions, and Figure 16, which represent the two-soliton solutions provided and represented through 3D, 2D, and contour plots.

Finally, understanding the dynamics and characteristics of the (3+1)-dimensional KP equation improves our understanding of the behavior of nonlinear waves in a variety of physical conditions and advances our understanding of wave phenomena in multidimensional systems.

5. Conclusions

The MSST and DT were used in this study to analyze the KP model in (3+1)-dimensional space using two alternative methodologies. The major goal of the study was to find many solitary wave solutions, one and two bright and dark soliton solutions and so on. This paper exhibits the originality of the MSST and DT application to the (3+1)-dimensional KP model. The obtained innovative soliton solutions not only improve the knowledge of soliton dynamics in higher-dimensional spaces but also the viability of the suggested approach. The results show the potential of the MSST and DT for further research on nonlinear wave phenomena and broaden the KP equation's applicability. The study's findings show that both methods are successful in obtaining the desired solutions. While the DT was utilized to produce two bright and two dark soliton solutions, the MSST was employed to provide dark, single, bright, exponential, and periodic solutions. The physical properties of the solutions were discussed, and the results were depicted using various visualization techniques. The obtained solutions are stable and can be used to describe various physical phenomena in different fields of research, such as fluid dynamics, plasma physics, and nonlinear optics. Overall, this study contributes to the understanding of the behavior of the KP equation in (3+1)-dimensional space and highlights the effectiveness of the MSST and the DT in obtaining different types of soliton solutions. Exploring the (3+1)-dimensional KP model and its soliton solutions has a wide range of potential applications and future research avenues. Researchers can further expand their comprehension of nonlinear wave phenomena while also revealing useful applications in disciplines like optics, fluid dynamics, and plasma physics by exploring these topics.

Author Contributions: Writing—review and editing, Formal Analysis, A.A.; Investigation, Methodology, Software, and Writing—original draft, S.J.; Supervision and Validation, M.N.; Conceptualization and Visualization, S.M.; Funding acquisition, and project administration L.F.I. All authors have read and agreed to the published version of the manuscript.

Funding: This research was funded by the University of Oradea.

Data Availability Statement: Not applicable.

Conflicts of Interest: The authors declare no conflicts of interest.

References

1. Jin, H.Y.; Wang, Z.A. Global stabilization of the full attraction-repulsion Keller-Segel system. *Discret. Contin. Dyn. Syst. Ser. A* **2020**, *40*, 3509–3527. [[CrossRef](#)]
2. Triki, H.; Wazwaz, A.M. On soliton solutions for the Fitzhugh–Nagumo equation with time-dependent coefficients. *Appl. Math. Model.* **2013**, *37*, 3821–3828. [[CrossRef](#)]
3. Guo, C.; Hu, J. Fixed-Time Stabilization of High-Order Uncertain Nonlinear Systems: Output Feedback Control Design and Settling Time Analysis. *J. Syst. Sci. Complex.* **2023**. [[CrossRef](#)]
4. Xie, X.; Huang, L.; Marson, S.M.; Wei, G. Emergency response process for sudden rainstorm and flooding: Scenario deduction and Bayesian network analysis using evidence theory and knowledge meta-theory. *Nat. Hazards* **2023**, *117*, 3307–3329. [[CrossRef](#)]
5. Rafiq, M.H.; Raza, N.; Jhangeer, A. Dynamic study of bifurcation, chaotic behavior and multi-soliton profiles for the system of shallow water wave equations with their stability. *Chaos Solitons Fractals* **2023**, *171*, 113436. [[CrossRef](#)]
6. Zhong, Q.; Han, S.; Shi, K.; Zhong, S.; Kwon, O. Co-Design of Adaptive Memory Event-Triggered Mechanism and Aperiodic Intermittent Controller for Nonlinear Networked Control Systems. *IEEE Trans. Circuits Syst. II Express Briefs* **2022**, *69*, 4979–4983. [[CrossRef](#)]
7. Guo, C.; Hu, J. Time base generator based practical predefined-time stabilization of high-order systems with unknown disturbance. *IEEE Trans. Circuits Syst. II Express Briefs* **2023**. [[CrossRef](#)]
8. Alotaibi, M.F.; Raza, N.; Rafiq, M.H.; Soltani, A. New solitary waves, bifurcation and chaotic patterns of Fokas system arising in monomode fiber communication system. *Alex. Eng. J.* **2023**, *67*, 583–595. [[CrossRef](#)]
9. Malik, S.; Hashemi, M.S.; Kumar, S.; Rezazadeh, H.; Mahmoud, W.; Osman, M.S. Application of new Kudryashov method to various nonlinear partial differential equations. *Opt. Quantum Electron.* **2023**, *55*, 8. [[CrossRef](#)]
10. Wang, L.; She, A.; Xie, Y. The dynamics analysis of Gompertz virus disease model under impulsive control. *Sci. Rep.* **2023**, *13*, 10180. [[CrossRef](#)]
11. Raza, N.; Arshed, S.; Wazwaz, A.M. Structures of interaction between lump, breather, rogue and periodic wave solutions for new (3+1)-dimensional negative order KdV-CBS model. *Phys. Lett. A* **2023**, *458*, 128589. [[CrossRef](#)]
12. Shakeel, M.; Shah, N.A.; Chung, J.D. Application of modified exp-function method for strain wave equation for finding analytical solutions. *Ain Shams Eng. J.* **2023**, *14*, 101883. [[CrossRef](#)]
13. Ali, A.; Ahmad, J.; Javed, S. Solitary wave solutions for the originating waves that propagate of the fractional Wazwaz–Benjamin–Bona–Mahony system. *Alex. Eng. J.* **2023**, *69*, 121–133. [[CrossRef](#)]
14. Rafiq, M.H.; Jhangeer, A.; Raza, N. The analysis of solitonic, supernonlinear, periodic, quasiperiodic, bifurcation and chaotic patterns of perturbed Gerdjikov–Ivanov model with full nonlinearity. *Commun. Nonlinear Sci. Numer. Simul.* **2023**, *116*, 106818. [[CrossRef](#)]
15. Liu, Q.; Peng, H.; Wang, Z. Convergence to nonlinear diffusion waves for a hyperbolic-parabolic chemotaxis system modelling vasculogenesis. *J. Differ. Equations* **2022**, *314*, 251–286. [[CrossRef](#)]
16. Malomed, B.A.; Mihalache, D. Nonlinear waves in optical and matter-wave media: A topical survey of recent theoretical and experimental results. *Rom. J. Phys.* **2019**, *64*, 106.
17. Cárdenas-Castillo, L.F.; Camacho-Guardian, A. Strongly Interacting Bose Polarons in Two-Dimensional Atomic Gases and Quantum Fluids of Polaritons. *Atoms* **2023**, *11*, 3. [[CrossRef](#)]
18. Chen, J.; Pelinovsky, D.E. Periodic waves in the discrete mKdV equation: Modulational instability and rogue waves. *Phys. Nonlinear Phenom.* **2023**, *9*, 133652. [[CrossRef](#)]
19. Gu, Y.; Zia, S.M.; Isam, M.; Manafian, J.; Hajar, A.; Abotaleb, M. Bilinear method and semi-inverse variational principle approach to the generalized (2+ 1)-dimensional shallow water wave equation. *Results Phys.* **2023**, *9*, 106213. [[CrossRef](#)]
20. Butt, A.R.; Raza, N.; Inc, M.; Alqahtani, R.T. Complexitons, Bilinear forms and Bilinear Bäcklund transformation of a (2+1)-dimensional Boiti–Leon–Manna–Pempinelli model describing incompressible fluid. *Chaos Solitons Fractals* **2023**, *168*, 113201. [[CrossRef](#)]
21. Wazwaz, A.M.; Alyousef, H.A.; El-Tantawy, S. An extended Painlevé integrable Kadomtsev–Petviashvili equation with lumps and multiple soliton solutions. *Int. J. Numer. Methods Heat Fluid Flow* **2023**, *33*, 2533–2543. [[CrossRef](#)]
22. Yang, S.X.; Wang, Y.F.; Zhang, X. Conservation laws, Darboux transformation and localized waves for the N-coupled nonautonomous Gross–Pitaevskii equations in the Bose–Einstein condensates. *Chaos Solitons Fractals* **2023**, *169*, 113272. [[CrossRef](#)]
23. Shen, Y.; Tian, B.; Zhou, T.Y.; Gao, X.T. N-fold Darboux transformation and solitonic interactions for the Kraenkel–Manna–Merle system in a saturated ferromagnetic material. *Nonlinear Dyn.* **2023**, *111*, 2641–2649. [[CrossRef](#)]
24. Yang, Y.; Xia, T.; Liu, T. Darboux transformation and exact solution to the nonlocal Kundu–Eckhaus equation. *Appl. Math. Lett.* **2023**, *141*, 108602. [[CrossRef](#)]
25. Alquran, M. Optical bidirectional wave-solutions to new two-mode extension of the coupled KdV–Schrodinger equations. *Opt. Quantum Electron.* **2021**, *53*, 588. [[CrossRef](#)]
26. Ablowitz, M.J. Nonlinear Waves and the Inverse Scattering Transform. *Optik* **2023**, *278*, 170710. [[CrossRef](#)]
27. Alquran, M. Physical properties for bidirectional wave solutions to a generalized fifth-order equation with third-order time-dispersion term. *Results Phys.* **2021**, *28*, 104577. [[CrossRef](#)]
28. Ran, X.; Wang, X.H.; Wei, T.F.; Qu, S.W.; Wang, B.Z. Inverse-Designed Superstrate for Arbitrary Shaped-Beam Radiation Pattern Based on Inverse Scattering Method. *IEEE Trans. Antennas Propag.* **2023**, *71*, 3828–3835.

29. Alquran, M. New interesting optical solutions to the quadratic–cubic Schrodinger equation by using the Kudryashov-expansion method and the updated rational sine–cosine functions. *Opt. Quantum Electron.* **2022**, *54*, 666. [[CrossRef](#)]
30. Ali, M.R.; Khattab, M.A.; Mabrouk, S.M. Optical soliton solutions for the integrable Lakshmanan-Porsezian-Daniel equation via the inverse scattering transformation method with applications. *Optik* **2023**, *272*, 170256. [[CrossRef](#)]
31. Wazwaz, A.M.; El-Tantawy, S.A. A new (3+1)-dimensional generalized Kadomtsev–Petviashvili equation. *Nonlinear Dyn.* **2016**, *84*, 1107–1112. [[CrossRef](#)]

Disclaimer/Publisher’s Note: The statements, opinions and data contained in all publications are solely those of the individual author(s) and contributor(s) and not of MDPI and/or the editor(s). MDPI and/or the editor(s) disclaim responsibility for any injury to people or property resulting from any ideas, methods, instructions or products referred to in the content.